# Dynamical Climatology

## A simple tropical coupled ocean - atmosphere model

by

G. R. Budin and M. K. Davey

DCTN 75

March 1989

Meteorological Office (Met. O. 20)
London Road
Bracknell
Berkshire RG12 2SZ

Dynamical Climatology Technical Note No. 75

# A SIMPLE TROPICAL COUPLED OCEAN-ATMOSPHERE MODEL

by

**G.R. Budin**

Hooke Institute for Atmospheric Research, Oxford

and

**M.K. Davey**

Met O 20 (Dynamical
Climatology Branch)
Meteorological Office
London Rd
Bracknell
Berkshire, U.K. RG12 2SZ

March 1989

Note: This paper has not been published. Permission to quote from it should be obtained from the Assistant Director of the above Meteorological Office Branch.

# CONTENTS


| | | Page |
|---|---|---|
| 1 | Introduction. | 4 |
| 2 | Description of the Atmospheric Model. | 5 |
| | 2.1 Introduction. | 5 |
| | 2.2 Dynamics. | 5 |
| | 2.3 Moist processes. | 8 |
| | 2.4 Land processes. | 12 |
| | 2.5 Boundary Layer Effects | 13 |
| | 2.6 Inclusion of atmospheric transients | 14 |
| 3 | Oceanographic Model. | 15 |
| | 3.1 Introduction. | 15 |
| | 3.2 Dynamics and Thermodynamics. | 15 |
| 4 | Coupling Procedure. | 17 |
| 5 | Numerical Procedures. | 17 |
| 6 | Model experiments. | 18 |
| | 6.1 Atmospheric model simulation of the observed tropical Pacific atmospheric circulation | 18 |
| | 6.2 Ocean model simulation of the 1982/83 ENSO | 18 |
| | 6.3 A coupled experiment - Pacific size basin. | 21 |
| | 6.4 A coupled experiment with realistic geometry. | 21 |
| 7 | Applications. | 23 |
| 8 | Further Developments. | 23 |
| REFERENCES | | 24 |

# Abstract

A simple coupled ocean - atmosphere model has been set up to study causes of equatorial inter - annual variability, such as that observed in the tropical Pacific in the form of the El-Niño Southern Oscillation. Vertical structure is reduced to one baroclinic mode in the atmosphere, and one active layer in the ocean. The shallow water equations on an equatorial beta plane govern the horizontal structure. The model is unique amongst simple models in having a moist, time dependent atmosphere: this enables the interaction of ENSO with shorter timescales (eg the 40 to 50 day wave) to be investigated. This report presents a detailed description of the model, together with selected brief results from experiments using the atmospheric and ocean models separately, and from coupled experiments.

# 1 Introduction.

The El Niño-Southern Oscillation phenomenon is a remarkable example of large inter-annual variability which disturbs the weather, and hence the environment and man's activities, over and around the Pacific basin (eg Canby, 1984). During and subsequent to the 1960's, research has established that ENSO is due to interactions of the ocean and atmosphere. Such research has involved both observational studies and a hierarchy of modeling studies. Simple coupled ocean-atmosphere models have recently been particularly useful in providing insight into possible instabilities in the Pacific climate system, and models are thus useful to other ENSO studies. Despite the intensive research effort on ENSO worldwide there is still no fully accepted theory for its onset, development, and decay.

The simple coupled tropical ocean-atmosphere model described here has been developed with an emphasis on some of the main processes thought to be most important to the interactions of the two fluids in the Pacific zone on long (inter-annual) time scales: ocean thermodynamics; atmospheric convective heating; land effects; and equatorial dynamics have been included. Our model includes a simple representation of the main convective-radiative state, but there is no interaction between model precipitation and radiation. This is a simplification which we find useful at this stage, but further development is needed to attempt to account for cloud - radiation feedbacks, which may also be of importance . With this model we are thus hoping to examine some of the possible mechanisms whereby the tropical Pacific ocean, surrounding land masses, and the tropical atmosphere may interact, producing large climate fluctuations such as those associated with the ENSO (Bjerknes, 1969). The model is based on extending the shallow water equations for both the atmosphere and ocean to account for the above processes, albeit in a highly simplified manner.

This report is organized as follows. We first describe the atmospheric and oceanic models (Sections 2 and 3) , and then the coupling procedure (Section 4). The numerical procedures are outlined in section 5. In section 6 we present some results of experiments with the model both uncoupled and coupled. Finally, we state some further applications of the model (Section 7) and discuss some potential improvements (Section 8).

# 2 Description of the Atmospheric Model.

## 2.1 Introduction.

The atmospheric model is based on that of Davey and Gill (1987) (hereafter referred to as DG). The vertical structure of the variables is specified to be that of the dominant vertical mode observed in the tropics - the first internal (baroclinic) mode (eg Yanai et. al., 1973). This vertical structure is shown in Fig. 1, where the vertical velocity $w$; potential temperature perturbation $\theta$ ; and heating $Q$, are maximum at the mid troposphere but zero at the surface and tropopause. Conversely, horizontal winds $(u, v)$ and pressure perturbation $P$ have opposite values at the surface and tropopause and are zero at mid-levels. Moisture $q$ is confined to the lowest layers of the atmosphere. Note that $\theta$ and $P$ are perturbations around fixed mean vertical profiles. The equations are of the linearized shallow water equation type, as first used by Matsuno (1966) and more recently by e.g. Gill (1980), Anderson and McCreary (1985a) (hereafter referred to as AMc) , Zebiak (1986), and Hirst (1986). The response to forcing by various prescribed heat source terms has been examined by various authors (Webster 1972, Anderson 1976, Gill 1980, Zebiak 1982, Heckley and Gill 1983, and Gill and Phlips, 1986). However the atmospheric latent or convective heating, $Q_l$, is ad - hoc in these models. Recently, modelers have taken into account the dependence of $Q_l$ on the wind convergence. Methods utilizing iterative feedbacks have been used by Webster (1982) and Zebiak (1986). It has become increasingly evident that in order to realistically model $Q_l$, moisture must be explicitly taken into account: a complex iterative method based on a water budget equation has been used by Weare (1986a), and extended by Weare(1986b), however a clearer approach was developed by DG. We note that the driving force of the towering cumulus convection in the tropics is moisture convergence in the unstable boundary layer (eg Holton, 1979 Ch 12, or Gill, 1982a, Ch11). The instability necessary for this is derived from the potential buoyancy of warm, moist low level air and hence depends strongly on the ambient SST. Thus there is a critical temperature ( needed to provide sufficient buoyancy) for widespread convection. The present model attempts to capture these processes in a simplified way ,with latent heat released into the mid troposphere when moisture reaches a critical relative humidity and is increasing.

## 2.2 Dynamics.

DG linearise the equations about a state of rest with stratification $\theta_0(z)$. There is a mid level potential temperature $\theta_s$, representing all diabatic heating other than latent heating , toward which the perturbation potential temperature $\theta$ is driven. The determination of $\theta_s$ is discussed later. The governing equations for the amplitudes of

the vertical modes (see DG for details) are

$$\begin{aligned}
\frac{\partial u}{\partial t} &= fv - \frac{1}{\rho_{00}}\frac{\partial P}{\partial x} - \epsilon u + \nu\nabla^2 u \\
\frac{\partial v}{\partial t} &= -fu - \frac{1}{\rho_{00}}\frac{\partial P}{\partial y} - \epsilon v + \nu\nabla^2 v \\
\frac{\partial \theta}{\partial t} &= w\frac{\partial \theta_0}{\partial z} - \epsilon\theta + Q_f + Q_l + \nu\nabla^2\theta \\
0 &= \frac{\partial u}{\partial x} + \frac{\partial v}{\partial y} + \frac{w}{H}
\end{aligned} \tag{2.1}$$

with

$f = \beta y$, the Coriolis parameter,

$\beta =$ the latitudinal gradient of $f$ taken constant at the equatorial value

$\epsilon =$ the equal Rayleigh friction and Newtonian cooling coefficients,

$H =$ the characteristic scale height (the tropopause is at height $\pi H$ as in Fig.1),

$\vec{u} =$ (u, v) the horizontal wind component at sea – level (in the boundary layer)

$\frac{\partial \theta_0}{\partial z} =$ the scale for background potential temperature change with height (a measure of dry static stability),

$Q_f = \epsilon\theta_s$ the fixed (prescribed) heating which drives $\theta$ towards a specified potential temperature distribution $\theta_s$ with a timescale of $\frac{1}{\epsilon}$ (the same rate as for Newtonian cooling)

$Q_l$, the latent heating, is given by $Q_l = mPr$, where

$Pr$ is the precipitation rate diagnosed from the moisture equation (see below),

$m = \frac{\rho_w L}{\rho_{mn} C_p H_0}$ is a moisture conversion factor,

$H_0$ is a latent heating projection factor.

If all latent heating released goes into the first baroclinic mode then $H_0 = 2H$.

$\rho_{mn}$ is a mean atmospheric density at the mid – levels where latent heating is released.

We take

$\rho_{mn} = \rho_{00} * 0.8$ with $\rho_{00}$ a mean atmospheric surface density.

$\epsilon u$ and $\epsilon v$ represent simply the net effect of boundary layer and other friction on the first baroclinic mode. $\epsilon\theta$ represents a relaxation due to radiative effects back toward the unperturbed state. As noted in Table 1a. these damping terms have a decay time scale of 2.3 *days*.

Assuming a linearization around a mean vertical profile, mid-level potential temperature $\theta$ and surface pressure $P$ are related by

$$\theta = -\frac{\theta_{00}}{\rho_{00} g H} P, \tag{2.2}$$

where

$\theta_{00}$ = a mean reference potential temperature
$g$ = gravity

The buoyancy frequency, N, is given by;

$$N^2 = \frac{g}{\theta_{00}} \frac{\partial \theta_0}{\partial z}$$

By considering $N$ constant, vertical modes have a simple sinusoidal shape as in Fig. 1.

These equations give a maximum internal gravity wave speed, $C = NH$; a horizontal distance scale given by the equatorial Rossby radius of deformation $a = \sqrt{\frac{c}{2\beta}}$, and a timescale, $\tau = a/c$. Typical values of all model parameters are listed in Table 1a, with physical constants in Table 1b and derived parameters (such as $C, a$, and $\tau$) in Table 1c.

It should be noted that the dynamic equations for the zonally asymmetric wind (derived from Eqns. 2.1) imply a Sverdrup balance between the stretching and horizontal advection of planetary vorticity. A study ( Sardeshmukh and Hoskins, 1985) has shown this to be a good approximation at low levels. However at higher levels the relative vorticity is also significant due to the greater vorticity advection, associated with the larger shear of the stronger winds. The current single baroclinic mode model does not include advective effects (except in the moisture equation) and hence cannot capture this aspect of the upper atmospheric circulation.

The atmospheric model can be seen from Eqn. 2.1 to be forced by a heating, $Q_f = \epsilon\theta_s$, which accounts for mid-level diabatic heating perturbation from sources

other than precipitation. It thus represents a perturbation from the basic stratification (enforced via the assumption of a constant basic lapse rate), due to a radiative/convective equilibrium. Thus $\theta_s$ should depend on the perturbation balance of long and short wave radiation, sensible heating, and sub-grid scale energy transfers. This relation is difficult to determine, and in the absence of a satisfactory simple theory, is taken (following DG) to be directly related to surface temperature, $T_s$, given by $SST$ over oceans and an effective surface temperature $T_e$ over land. Specifically we take

$$\theta_s = T_s - T_s^{ref}, \tag{2.3}$$

with $T_s^{ref} = 26.5$ °C as a convenient reference tropical surface temperature (ie that which is in balance with the basic state). The quantity $\theta_s$ may also be thought of as a thickness perturbation between the upper and lower troposphere. It seems reasonable that even in the absence of precipitation, this thickness would be larger over warmer surfaces. This parameterization is no doubt a gross simplification, since it effectively assumes a constant lapse rate in the absence of precipitation, but shall suffice for our present purposes.

## 2.3 Moist processes.

The moisture budget takes the simple form

$$\frac{\partial q}{\partial t} + Pr = -\vec{\nabla}.(\vec{u}q) + E + \nu\nabla^2 q \tag{2.4}$$

where $q$ is the total column moisture. The evaporation is $E$ , the form of which shall be discussed below. Note that a diffusion term is included. Precipitation $Pr$ is determined by this moisture balance. If we set $M$ to be the right hand side of Eqn. 2.4 then $M$ is the local rate of increase of total moisture, ie

$$M = \frac{\partial q}{\partial t} + Pr.$$

Previously DG assumed that precipitation occurred only if $q$ reached its saturation value, $q_s$, above which any further moisture increase is rained off. Here we expand on that by allowing precipitation to occur whenever the relative humidity ($RH$) exceeds a threshold, $RH_c$. This parameterization is an attempt to account for the difficulties in resolving sub - grid scale precipitation. Clearly precipitation would start at some places in a grid box before the whole box becomes saturated. We take the precipitation to be zero for relative humidities that are sub - threshold, increasing linearly to a maximum when saturation is reached. Hence we have a partitioning between moisture increase and rainfall

$$\begin{aligned} &\frac{\partial q}{\partial t} = (1-\sigma)M, \ and \\ &Pr = \sigma M, \end{aligned} \tag{2.5}$$

with

$$\sigma = \begin{cases} \dfrac{q - q_c}{q_s - q_c}, & \text{if } q > q_c \text{ and } R > 0; \\ 0, & \text{otherwise.} \end{cases}$$

Here $q_c = q_s RH_c$ is the threshold moisture content, and $q_s$ is the saturation moisture value. For a given temperature $T, q_s$ can be determined by assuming a constant tropical lapse rate of 6.5 °C per kilometer and taking perturbations of the observed saturation vapour pressure versus temperature relationship around a representative tropical temperature of 27 °C (in similar fashion to Gill, 1982b), to obtain

$$q_s = q_f e^{(0.06(T_s - 27))} \tag{2.6}$$

with $q_f = q_s$ at 27°C (see Table 1a).

During a time $\delta t_a, \sigma$ is changing and indeed may become greater than zero so that precipitation commences. To make the finite difference model consistent with the above formulation , Eqn. 2.5 is integrated analytically for the model time step, $\delta t_a$, (during which time M is constant). Integrating from time $t$, when $q = q_l$, to time $t + \delta t_a$, when $q = q_n$, gives

$$q_n = q_l + M\delta t_a \tag{2.7}$$

if there is no rain during the model timestep, otherwise

$$q_n = q_b e^{(\alpha \delta t')} + q_s(1 - e^{(\alpha \delta t')}) \tag{2.8}$$

where,

$$\delta t' = \begin{cases} \delta t_a - \dfrac{q_c - q_s}{M}, & \text{if } q_l < q_c; \\ \delta t_a, & \text{otherwise,} \end{cases}$$

is the amount of time during the timestep for which precipitation takes place,

$$\alpha = \frac{M}{(q_s - q_c)},$$

and

$$q_b = \begin{cases} q_c, & \text{if } q_l < qc; \\ q_l, & \text{otherwise.} \end{cases}$$

This formulation ensures that the moisture content never becomes supersaturated, and gives a smooth onset of precipitation ( as opposed to the on-off 'jump' used by DG). Evaporation is given a bulk aerodynamic form;-

$$E = (E_0 + E_v|v|)q_s(1 - RH_b) \tag{2.9}$$

where $E_v$ is a wind speed dependent evaporation rate, derived from that of Bunker (1976), and $E_0$ is a minimum evaporation rate, to account for evaporation associated with high frequency wind variability which the model does not simulate. $RH_b$ is given by

$$RH_b = \begin{cases} RH, & \text{if } RH < RH_c; \\ RH_c & \text{otherwise.} \end{cases}$$

Thus the humidity dependent term is prevented from approaching zero as saturation is reached. The values of $E_v$ and $E_0$ given in Table 1a: for a wind speed of 5 $m/sec$ at 28 °C and relative humidity of 75% the evaporation rate is about $3mm/day$, a reasonable tropical value (see eg Weare, Strub and Samuel, 1980).

The model precipitation is an important model parameter and strongly influences model stability, so let us consider the effects of latent heating in more detail. We note that evaporation is small in regions of rain (see Eqn. 2.9): similarly we may assume that $\nabla q$ and $q_t$ will also be small in rainy regions (this will be generalised later). Neglecting diffusion and combining Eqn. 2.4 with the continuity equation in Eqn. 2.1, we have approximately

$$Pr = \begin{cases} \dfrac{\sigma q w}{H}, & \text{if } w > 0 \text{ and } \sigma > 0; \\ 0, & \text{otherwise.} \end{cases}$$

Substituting this expression into the thermodynamic equation (Eqn. 2.1 for $\dfrac{\partial \theta}{\partial t}$ ) gives, again neglecting diffusion, for precipitating regions

$$\frac{\partial \theta}{\partial t} = -w\frac{\partial \theta_0}{\partial z} + \frac{\sigma q w m}{H} + \epsilon(\theta_s - \theta)$$

or,

$$\frac{\partial \theta}{\partial t} = -w\frac{\partial \theta_e}{\partial z} + \epsilon(\theta_s - \theta)$$

Here $\dfrac{\partial \theta_e}{\partial z}$ is the effective moist static stability ( the gradient of a suitable equivalent potential temperature) given by,

$$\frac{\partial \theta_e}{\partial z} = \frac{\partial \theta_0}{\partial z}\left(1 - \frac{\sigma q m}{H\dfrac{\partial \theta_0}{\partial z}}\right)$$

Defining $\Gamma_s$ as the ratio of the static stability in precipitating regions to that in dry

regions , ie ,

$$\Gamma_s = \frac{\frac{\partial \theta_e}{\partial z}}{\frac{\partial \theta_0}{\partial z}}$$

then we have $\Gamma_s = 1 - \hat{q}$, where,

$$\hat{q} = \kappa q \left(\frac{q - q_c}{q_s - q_c}\right) = \kappa q_s RH \left(\frac{RH - RH_c}{1 - RH_c}\right), \quad \text{and}$$

$$\kappa = \frac{m}{H \frac{\partial \theta_0}{\partial z}}$$

$\hat{q}$ is a non - dimensional stability parameter equivalent to that used by Gill (1982b). It represents the ratio of latent heating to adiabatic cooling in areas of upward motion. $\hat{q}$ varies with humidity and temperature in a fashion shown in Figs. 2a and 2b, respectively, increasing smoothly from the dry value (zero) at sub-critical moisture levels , to $q_s$ at saturation. Indeed the maximum value of $\hat{q}$ is an important model parameter, since should it exceed 1, $\Gamma_s$ becomes negative, and moist buoyancy 'waves' become stationary and unstable, growing most quickly at the smallest scales. These structures resemble tropical cyclones and have been discussed by Gill (1982c). With the model parameters as in Table 1 we find $\hat{q}$ reaches 1 at a temperature of 29.8°C (see Fig. 2b), which is rarely exceeded on the time and space scales of interest here. This implies that although convective overturning does occur in tropical precipitating systems, these are localized, and on the large space and long time scales we are modelling we expect the tropical atmosphere on average to be moist stable for deep convection.

The above stability analysis assumed evaporation and $q$ derivatives to be small in precipitating regions. If these are high , it is possible that the latent heating could still be sufficient for the model to become unstable ($\hat{q} > 1$). This can be seen by generalizing the above arguments for any precipitation rate. Using Eqns. 2.4 and 2.1 we find

$$\hat{q} = \frac{mPr}{w \frac{\partial \theta_0}{\partial z}}$$

with Pr given by the full expression of Eqn. 2.4. In practice we find for realistic precipitation rates (for temperatures less than about 30 °C) the ratio of precipitation rates to vertical velocity is still insufficient to make $\hat{q}$ exceed 1.

The previous formulation of DG gave an abrupt decrease in stability upon reaching saturation (rather than the smooth change found here). This variation in effective stability means propagating features slow down in precipitating regions (as in Gill,

1982b). This may account for the slow phase speed of the 40/50 day wave as compared to the first baroclinic Kelvin mode phase speed, whose vertical structure it resembles (Swinbank, Palmer and Davey, 1988). In the present model there will be a range of phase speeds for such a wave, depending on the humidity, but also on the saturation moisture level.

The present model has atmospheric heating, $Q$, composed of two parts,

$$Q = Q_f + Q_l,$$

with $Q_f$ specified but $Q_l$ determined internally by the model moisture balance. Most previous models have used only a fixed heating similar to $Q_f$, dependent only on SST (though sometimes in a non-linear form), but with much larger coefficients. Thus those models are attempting to model latent heat release purely as a function of SST: here we interpret $Q_f$ as a background radiative-convective heating and determine latent heating $Q_l$ explicitly. To show the difference in heating that results, Fig. 3 shows $Q_f$ and $Q_l$ as a function of $SST$ ($Q_l$ being derived from a model run in wet regions) and for the linear heating profile of Hirst (1986, and 1988) and the ramp heating function of AMc. Note that in this figure heating has been rescaled to be in the units used by AMc. In the present model latent heating dominates the fixed heating and has a general trend to increase with SST in a fashion more like the Hirst heating profile than that of AMc.

The modification of the forcing $\theta_s$ and moist processes over land are now discussed.

## 2.4 Land processes.

Over land we need an effective surface temperature $T_e$ to determine the surface saturation moisture and mid-level background heating $Q_f$. Here we specify $T_e$ to depend on the specified seasonal heating of the continents. This is a simple parameterisation avoiding the need for a surface energy balance equation normally used to determine the surface temperature in more complete models. Such a method is beyond the scope of the present model formulation, but could be incorporated at a later date. In accounting for the annual solar cycle we aim to represent the seasonal reversal of the land/ocean heating difference which drives the monsoon circulation.

We choose a simple form for $T_e$ , quadratic in latitude, with the maximum following the annual cycle of the sun, namely;-

$$T_e = (lt_{eq} - lt_{bn})(1 - ((y - ymh)/ymaxa)^2) + lt_{bn}$$

where
$lt_{eq}$ is the maximum temperature, at the equator at equinox,

$lt_{bn}$ is the boundary temperature at equinox,
$y$ is the latitude,
$ymaxa$ is the highest latitude in the atmospheric model,
$ymh$ is the latitude of maximum heating which varies with the day of the year, d, as ;-

$$ymh = 23.3cos(\frac{(d' - 180)\pi}{180}),$$

with

$$d' = d + 10 - 360(int(\frac{d}{360}))$$

so that the model solstices occur at days 170 and 350 in a 360 day model year. Note we have ignored the effect of land heat storage which delays the heating maximum to be later than the solar heating maximum.

We expect the above simple parameterization of heating over land to produce only a rough approximation to the observed trade wind and monsoonal flow. There is no variation in the longitudinal direction, so we have neglected effects of mountain ranges, variations in surface characteristics , etc. The main aim for the purposes of this model is to produce reasonable values for the model fields near the land/ocean boundaries. An alternative approach would be to make the model an anomaly around the annual cycle. The annual cycle can be defined by inverting Eqns. 2.1 using climatological monthly winds to determine $\theta_s$ for each month (the $\chi$ problem discussed by Sardeshmukh and Hoskins, 1985).

Evaporation over land needs to be modified to account for land dryness. This is achieved by multiplying the evaporation by a soil moisture availability factor given by $\frac{SM}{SM_d}$ where SM is the soil moisture given by the integral of the surface water flux,

$$SM = \int (Pr - E)dt$$

and $SM_d$ is the maximum soil moisture, above which all precipitation 'runs off' and is lost from the model. This method of handling the moisture balance over land is the familiar 'bucket' method with $SM_d$ the bucket depth.

## 2.5 Boundary Layer Effects

The atmospheric model used here ignores boundary layer effects. Since we are really interested in modelling the wind over the ocean surface (and hence in the maritime boundary layer) it is of relevance to comment on our attempts to include a boundary

layer in the model. We note that the model damping time (see Table 1), 3 *days*, is taken as being representative of the frictional damping experienced by the model baroclinic mode due primarily to boundary layer frictional processes. We note that a damping time scale of about 1 *day* is more appropriate for the boundary layer itself. Hence a simple boundary layer representation was attempted by including a 1km fixed height layer with increased linear friction (corresponding to a 1 *day* damping rate). When forced with observed SSTs the model simulated stronger and more realistic meridional winds (a deficiency in the normal model, see Section 6.1). However, grossly unrealistic equatorial precipitation patterns were found. In a recent paper Lindzen and Nigam (1987), using a simple but dry atmospheric boundary layer model, encountered similar difficulties. They removed these by including even stronger damping (30 minutes), and allowing the boundary layer height to vary, so allowing rapid pressure adjustment. However they do not include convective heating in their model, and this makes their case simpler than the present model. It is difficult to see a consistent model formulation of the type Lindzen and Nigam used which can combine their boundary layer model with a moist atmospheric model of the free atmosphere. This is due to difficulties in matching boundary conditions at the interface.

We believe that inclusion of a boundary layer would not alter the modes of the coupled model (since latent heating in the middle troposphere dominates boundary layer sensible heating), which is the main focus of our attention. Further we note that in reality (see eg. Oort, 1983) the boundary layer and 'free atmosphere' show strong coupling in some areas (eg, the central Pacific) and none in others (eg the south-east Pacific). Such complex behaviour is beyond the scope of simple models and indeed is a challenge for general circulation models.

## 2.6 Inclusion of atmospheric transients

The atmospheric model described above is incapable of simulating atmospheric transients, reaching the same steady state (within 10 or so days) for a given SST forcing, regardless of initial conditions. Recently it has been noted (eg Lau and Chan, 1988) that intraseasonal variability (which is dominated by the '40/50 day' wave ) may be of importance in affecting the ENSO phenomena (on the inter-annual time-scales). The '40/50 day' wave appears in the atmospheric model here as a moist Kelvin wave which is preferentially enhanced when for example, a small stochastic 'white noise' forcing is included in the mid-level potential temperature equation (see Davey, 1989). Inclusion of a similar forcing has been used in the coupled model to investigate the interaction of the '40/50 day' wave and ENSO type modes (see Davey and Budin, 1989 for details and results using a restricted domain).

# 3 Oceanographic Model.

## 3.1 Introduction.

In a similar way to the previously discussed atmospheric models, oceanographic simple models have also been developed using simple shallow water equations. A complete review of equatorial ocean modeling can be found in McCreary (1985). The success of the linear shallow water model of Busalacchi and O'Brien (1981), with one active layer representing the region above the thermocline, in modeling the sea surface height shows that such models correctly represent the basic equatorial dynamics in most of the Pacific. For coupling to atmospheric models one also requires the $SST$ field, and hence a thermodynamic model is needed. A completely satisfactory thermodynamic model is difficult to achieve in simple models. Nevertheless, AMc have utilized a thermodynamic equation which includes parameterization of entrainment at the base of the mixed layer (upwelling), wind mixing, and a Haney heat flux into the layer from the atmosphere.

Recently, more physically realistic 'intermediate' mixed layer thermodynamic models have been developed (Cane, Zebiak and Dolan, 1986, and Andrich, 1988). These include directly (but in a simplified fashion) the oceanic heating components; short wave radiation (which may depend on cloud cover), long wave radiation , evaporative cooling, sensible heat transfer etc. We plan to extend our current model (described below) in such a fashion at some stage in the future.

## 3.2 Dynamics and Thermodynamics.

The AMc model is a generalization of the shallow water or reduced gravity equations which includes simple thermodynamics. Fig. 4 shows a vertical cross - section of the model. The model equations are

$$\begin{aligned} \frac{\partial(hu_o)}{\partial t} &= fhv_o - \frac{1}{\rho_w}\frac{\partial P}{\partial x} - \vec{\nabla}.(\vec{u}_o hu_o) + \nu\nabla^2(hu_o) + \frac{\tau_x}{\rho_w} \\ \frac{\partial(hv_o)}{\partial t} &= -fhu_o - \frac{1}{\rho_w}\frac{\partial P}{\partial y} - \vec{\nabla}.(\vec{u}_o hv_o) + \nu\nabla^2(hv_o) + \frac{\tau_y}{\rho_w} \end{aligned} \tag{3.1}$$

$\vec{u}_o = (u_o, v_o)$ is the ocean current,
h is the upper layer thickness,
$\vec{\tau} = (\tau_x, \tau_y)$ is the wind stress,

$P = \frac{1}{2}\alpha\rho_w g h^2 T$, is the layer potential energy,
$T$ is the temperature excess of the surface layer over the deep inert layer,
$\nu$ the viscosity coefficient (dissipation)
$\rho_w$ the constant density of deep layer water
$\alpha$ the thermal expansion coefficient of water.
The density of the upper layer $\rho_u$ is $\rho_u = \rho_w(1 + \alpha T)$
All model parameters are listed in Table 2, together with physical constants and derived model parameters.

Actual sea surface temperature ($SST$) is related to the upper layer temperature excess, T, by

$$SST = T + T_0.$$

The lower layer temperature, $T_0$ is chosen to be 17 °C, so that the $SST$ will have a maximum of around 29 °C.

The continuity and thermodynamic equations are

$$\begin{aligned} \frac{\partial h}{\partial t} &= -\vec{\nabla}.(\vec{u}_o h) + \frac{2\delta}{hT} - w + \gamma\frac{(T - T^*)}{T} \\ \frac{\partial T}{\partial t} &= -\vec{u}_o.\vec{\nabla}T + \frac{2}{h}[\gamma(T^* - T) - \frac{\delta}{h}] \end{aligned} \tag{3.2}$$

where $w$ is a specified constant background upwelling (presumed driven by a large scale deep thermohaline circulation), and $\delta$ is a wind mixing term. Following AMc this is given to be

$$\delta = \frac{\delta_o}{h},$$

with $\delta_o$ a specified constant.

The surface heat flux into the ocean is $Qs = \rho_w C_p \gamma(T^* - T)$ (cf Haney, 1971), with a typical timescale $\frac{h}{\gamma}$ of 270 days along the equator. For this Haney forcing $T^*$ is an equivalent temperature chosen such that the flux proportional to $T^* - T$ represents a linear (in T) perturbation from equilibrium encompassing the effects of varying solar radiation, long wave radiation, sensible and latent heat,(see eg Haney, 1971 and Wells and King-Hele, 1989). (Note $T$ is always less than $T^*$ , so there is always heat input to the ocean). As in AMc $T^*$ is taken to vary only with the cosine of latitude, from a value of 14 at the equator to 6 at 31° from the equator. In reality $T^*$ would depend on many factors; we use this approximation for simplicity. Note that, as with $T$, $T^*$ is here measured relative to the deep ocean for convenience: $T_0 = 17$ should be added to the above values to obtain values in °C.

The approximate effect of these thermodynamic processes can be gauged by ignoring horizontal advection: then the model would relax to a state with

$$\bar{T} = \frac{\gamma T^*}{\gamma + w}. \tag{3.3}$$

With parameters given as in Table 2, $\bar{T}$ varies from 12 ($SST = 29°C$) at the equator to 5 ($SST = 22°C$) at the boundary (31°latitude). The corresponding thermocline depth is

$$\bar{h} = \sqrt{\frac{\delta_o(\gamma + w)}{\gamma w T^*}}, \tag{3.4}$$

which increases from 76m at the equator to 117m at the boundary. $\bar{T}$ and $\bar{h}$ are shown as a function of latitude in Fig. 5.

No normal or tangential flow is allowed along the boundaries. Kelvin wave damping is included near the north and south boundaries, ie in the h equation within 450km of the boundaries a term of the form $-\kappa(h - \bar{h})$ is added, with $\kappa$ decreasing linearly from about 1/46 days at the boundary to be zero 450km away. $\bar{h}$ is the mean depth defined above.

# 4 Coupling Procedure.

Both the component models are time dependent and exchange wind stress and heat every 5 days. The instantaneous values are used rather than an average, since we are generally concerned with phenomena which have a long time scale and hence vary little in 5 days. When this assumption may not be valid (eg during a 40/50 day wave study) the interval between coupling can be readily decreased. Following AMc, a simple linear wind stress has been prescribed;

$$\vec{\tau} = \rho C_d \vec{u} \tag{4.1}$$

$C_d$ a modified drag coefficient, and
$\vec{u}$ the atmospheric wind velocity.
This stress law has been linearised about a speed of 5m/sec for analytic convenience initially, though this constraint could be dropped. Note that for wind speeds over 5m/sec this stress law will result in smaller stresses than the normal quadratic law.

# 5 Numerical Procedures.

The atmospheric model is solved on an Arakawa C-grid ( Fig. 6), with resolution set at $\delta x_a = 4°$, and $\delta y_a = 4°$. The model uses a predictor - corrector time stepping scheme, with time step $\delta t_a = 1200$ seconds ( 20 minutes). The ocean model is also solved on a C-grid (Fig. 7) with resolution set at $\delta x_o = 1°$, and $\delta y_o = 1°$. A leap-frog time stepping scheme with time step $\delta t_o = 3$hrs is used.

The models exchange $\vec{\tau}$ and $SST$ every 5 days. A linear interpolation routine is used to transfer these quantities between model grids.

In the next section we describe experiments using the component models separately, and the coupled model both in a Pacific size basin and finally with realistic global geometry.

# 6 Model experiments.

## 6.1 Atmospheric model simulation of the observed tropical Pacific atmospheric circulation

In an attempt to see how well the atmospheric model could simulate the observed tropical Pacific circulation, the model was run with observed mean monthly SSTs and the land forcing described in Section 2.4 for an idealized tropical Pacific basin. The model winds and precipitation for January and July are presented in Figs. 8 and 9 (taken from Budin and Davey, 1988). These can be compared with observations, reproduced in Figs. 10 and 11 (from Weare, Strub and Samuel, 1980 for wind and Shea, 1986 for precipitation). The model winds show the basic observed pattern of predominantly easterly trade winds in most areas, but are more zonal than observed. The monsoonal reversal in the west Pacific is simulated, though the seasonal reversal in the 10 °N eastern coastal region is more pronounced than in reality . The model precipitation correctly shows a stronger South Pacific Convergence Zone in the southern summer. The Inter-Tropical Convergence Zone is simulated but much weaker than observed, particularly in July. This is related to a lack of boundary layer effects which result in stronger meridional flow (see section 2.5). Over land the ITCZ follows the solar heating maximum, though less confined to coastal areas than observed. This is not surprising since the model does not include topographic effects, and for this experiment a smoothing was applied to $\theta_s$ in coastal areas.

Thus we see the atmospheric model is able to simulate in a broad sense the most significant aspects of the circulation.

## 6.2 Ocean model simulation of the 1982/83 ENSO

The ability of the ocean model to simulate an observed ENSO event was studied by forcing the ocean model alone with observed monthly winds (subjectively analysed as in Goldenburg and O'Brien, 1981, and often referred to as FSU winds) from January 1980 to December 1983. This experiment was performed at 2 °by 2 °resolution with a viscosity and diffusion of 4000 $m^2/sec$, and with ocean thermodynamic parameters as initially used by AMc (slightly different from those listed in Table2).

The model shows warm water moving eastwards in response to the westerly winds, commencing in July 1982, with the warmest waters reaching a maximum eastward longitude almost a year later (Fig. 12a) . Whilst this timing is similar to that observed (Fig. 13, after Reynolds, personal communication) the model fails to predict very warm water (over 28 °C) east of 150 °W during the peak of the ENSO event. This failure is perhaps related to underestimated advective effects as the currents produced by this model are somewhat less than those found in general circulation model hindcasts of the 1982/83 ENSO event. The maximum eastward current around October 1982 was about 0.15 $m/sec$ in the present model compared to over 1 $m/sec$ in GCM hindcasts (Gordon, personal communication). These weak currents were most likely due to a combination of a generally weaker stress used in the present study than in the GCM simulations, and the poor horizontal resolution (with associated high viscosity) used here. Also the single layer model has weak currents due to depth averaging. Experiments with higher resolution and stronger stress were carried out, but these readily became unstable as discussed below.

The thermocline depth development (Fig. 12b) shows the position of maximum depth moving eastwards during the second half of 1982 and early 1983, slightly leading the position of warmest water. However it is clear that the model produces unrealistic thermocline gradients: for instance between 170 °W and 120 W during the latter half of 1982, and near 180 °E late in 1983, the thermocline tilts by up to 80m in 10 °of longitude, much larger than occurs in reality (however no continuous observations are available to directly compare with for this period) . If a quadratic stress law is used the model becomes unstable in such regions, producing strong Kelvin wave fronts (and off-equatorial solitary Rossby gyres) of the type noted by Greatbatch (1985). This problem is exacerbated in this model as the following argument shows.

In a steady state, neglecting currents, the equatorial equilibrium thermocline depth gradient varies as

$$\frac{\partial h}{\partial x} = \frac{\tau_x}{\rho c^2}.$$

Because this model is non-linear and also is free to select its own thermocline depth, the mean depth value (and hence $c$) is not fixed. This contrasts with most other single layer models which have been reported, including Busalacchi and O' Brien (1981), and Greatbatch (1985). Here $c$ varies locally according to the local depth and temperature;

$$c^2 = g\alpha T h,$$

which can give very low wave speeds, and hence strong thermocline depth gradients for a given stress. Fig. 14 shows a plot of $c$ along the equator for the ocean model in September, 1982. This shows that $c$ varies from about 1.6 $m/sec$ to 0.7 $m/sec$, and in the latter regions the equatorial thermocline slope can become unreasonably large when wind stress is strong. Of course we could artificially fix $c$ at a constant value, but we find in this case (not shown) that the $SST$ simulation suffers.

Another way of looking at this is that when the model thermocline is shallow excessive energy is going into the single mode modelled here, when in reality it should be distributed between the first two modes. Indeed it has been shown that a first baroclinic mode Kelvin wave travelling through a shoaling thermocline transfers appreciable energy to the second baroclinic mode in the east Pacific (Gill and King, 1985). Such a mechanism is not accounted for in the present model and hence can lead to excessive energy building up (in the form of strong horizontal gradients in the thermocline).

This experiment and others we have carried out varying the thermodynamic parameters of the ocean model show that the AMc ocean model is limited in its ability to produce both realistic SST and thermocline depth simultaneously. The parameters chosen by us in the present experiment were chosen to best reproduce the observed SST development. Yamagata and Masumoto (1989) altered the original ocean model parameters from that used by AMc so as to best reproduce the ocean thermocline and propagation speed. However it was found (Yamagata, personal communication) that the model SSTs were unrealistic, with a very small gradient across the Pacific when forced with the normal easterly wind pattern.

The inability of the AMc ocean model to successfully simulate both SST and thermocline depth simultaneously is hardly surprising: the model contains only three highly idealized thermodynamic processes against the numerous and more complex

processes operating in GCM's and in reality. Its main usefulness is in the study of coupled processes, rather than accurate hindcasting using observed winds.

A further model deficiency can be seen in both the thermocline depth and $SST$ in the far western Pacific, where large gradients are simulated. This seems to be associated with the idealised coastline the model uses in the west Pacific: other experiments (not shown) with a higher resolution model and more realistic coastline did not show this feature.

## 6.3 A coupled experiment - Pacific size basin.

Here we describe a simple coupled experiment with a rectangular bounded basin ocean the width of the Pacific and an overlying atmosphere. The atmosphere is periodic in the east-west direction with period equal to the ocean basin width, and there is no land. The model was initialized by first running the ocean model alone with an easterly wind patch located in the basin centre near the equator with a maximum speed of 10 $m/sec$ for 100 *days* , starting from the steady solutions, Eqns. 3.3and 3.4. This initial 'warm up' of the ocean is done in order to trigger the model to produce a 'warm event' disturbance soon after coupling. Further experiments have shown the model behaves in a similar fashion regardless of the presence or absence of this initial warming up of the ocean.

The models were then coupled and exchanged $SST$ and wind stress every 5 *days*. Fig 15. shows the development of $SST$ and precipitation. The model develops instabilities which propagate eastwards across the ocean basin with a period of about 4 years. Precipitation overlies high $SST$ (above about 26 °C). The model response bears a strong resemblance to the so-called mode IV found in the linear model analysis of Hirst (1986). This mode is a oceanic Kelvin wave modified by coupling, and shows a high correlation between development of increased $SST$, increased atmospheric heating, and a deepened thermocline. Hirst's analysis was linear and did not include moisture: atmospheric heating was fixed to be proportional to $SST$. In our case a dynamic moisture budget determines precipitation and hence most of the atmospheric heating (as in section 2.), but this has made little difference to the type of response obtained.

The model instability has some features in common with that observed, namely eastward propagation and a strong matching of high precipitation, high $SST$, and a deep thermocline. However the time for the model disturbance to move cross the Pacific basin (about 4 years) is quite a lot longer than that observed (several months), and agrees more closely with the return period of ENSO events (2 to 7 years). Further experiments have shown that the period of the instability developed by the model

decreases with increasing coupling coefficients ($C_d$ , $Q_f$ and $Q_l$) in broad agreement with Hirst (1986) and (1988).

## 6.4 A coupled experiment with realistic geometry.

Here we describe an experiment with the model using real world geometry, though with no perturbation forcing over land. Hence we took $lt_{eq} = lt_{bn} = T_s^{ref}$ (26.5 $^\circ C$) so that $\theta_s$ is zero over land. The ocean model was started from the equilibrium temperature and depth (as in Eqns. 3.3 and 3.4). The atmospheric model was initially run for 15 days with the forcing fixed. The models were then coupled and run for 20 years, exchanging information every 5 days . The development of near equatorial precipitation is shown in Fig. 16. The model undergoes regular oscillations confined to that Pacific basin, though with some small associated fluctuations in the Atlantic and Indian basins.

Further experiments indicate that the development of disturbances within the model is strongly affected by land heating. If the effective land temperature along the equator, $lt_{eq}$ is raised to 28.5 °C the main precipitation belt is confined to over and near the land masses, and no oscillations develop. Conversly, if $lt_{eq}$ is decreased to 24.5 °C, model disturbances are damped and after a few years the model settles to a steady ENSO like state with warm water and precipitation shifted eastwards to the central to eastern Pacific. This is a clear indication that land heating, and in particular the development of widespread convection over the Asian-Australian region, influence the coupling of the ocean and the atmosphere over the Pacific. This is something noted by AMc (and Anderson and McCreary 1985b), Yamagata (1987), and Yamagata and Masumoto (1989) but not included explicitly in many other works (Hirst 1988, Battisti 1988, etc). The results found here suggest other influences outside those proposed by Battisti (1988) and Hirst (1988) which rely on equatorial ocean wave dynamics and the coupling of the atmosphere with the ocean only. Here we find that simple model behaviour is intrinsically a land-ocean-atmosphere coupling process.

# 7 Applications.

This report describes a simple coupled ocean - atmosphere model aimed at simulating the major aspects of the ENSO cycle. The model is being used to understand the processes involved in ENSO, and is a useful adjunct to concomitant research being carried out in the Hooke Institute and Meteorological Office using fully coupled GCM's.

Questions which may be addressed with the model in the future include;-
(1) What is the role of moisture in affecting ENSO development and behaviour ?
(2) What is the role of short time scale atmospheric fluctuations (eg the 40/50 day wave) in affecting the initiation and decay of an ENSO event ?, and,
(3) What is the role of the annual cycle and land processes in affecting the evolution of unstable tropical coupled ocean - atmosphere modes?

# 8 Further Developments.

The model developed and used here is designed as a baseline model with which initial coupled experiments can be performed. However future refinements are desirable to increase the realism of the model. These include;-

(i) Developing a higher resolution ocean model with a variable grid and so lower damping. This will enable closer monitoring of equatorial waves shown to be important in some simple coupled models (Battisti, 1988).

(ii) Including more realistic thermodynamics in the ocean model. Such a model could use Kraus-Turner mixing and incorporate cloud-radiation feedbacks.

(iii) A more realistic atmospheric model, using a multi-level atmosphere including a boundary layer.

## References


Anderson, D.L.T., 1976: The low-level jet as a western boundary current. *Mon. Wea. Rev.*, 104, 907-921.

Anderson, D.L.T. and J.P. McCreary, 1985a: Slowly propagating disturbances in a coupled ocean-atmosphere model. *J. Atmos. Sci.*, 42, 615-628.

Anderson, D.L.T. and J.P. McCreary, 1985b: On the role of the Indian ocean in a coupled ocean-atmosphere model of El Niño and the Southern Oscillation. *J. Atmos. Sci.*, 42, 2439-2442.

Andrich, P., 1988: Simulations of the sea surface temperature with a 2 layer model of the tropical oceans. Sub. to *J. Geophys. Res.*

Battisti, D.S., 1988: Dynamics and thermodynamics of a warming event in a coupled tropical atmosphere-ocean model. Sub. to. *J. Atmos. Sci.*

Bjerknes, J.A., 1969: Atmospheric teleconnections from the equatorial Pacific, *Mon. Wea. Rev.*, 97, 163-172.

Budin, G.R., and M.K. Davey, 1988: A simple model simulation of the atmospheric circulation over the tropical Pacific . *Trop. Ocean-Atmos. Newsletter.*, 44, 4-7.

Bunker, A.F., 1976: Computations of surface energy flux and annual air - sea interaction cycles of the north Atlantic ocean. *Mon. Wea. Rev.*, 104, 1122-1140.

Busalacchi, A. and J.J. O' Brien, 1981: Interannual variability of the equatorial Pacific in the 1960's. *J. Geophys. Res.*, 86, 10901-10907.

Canby, T.Y., 1984: El Niño's ill wind. *Natl. Geogr.*, 165,144-183.

Cane, M.A. and S.E. Zebiak and S.C. Dolan, 1986: Experimental forecasts of El Niño. *Nature* , 321, 827-832.

Davey, M.K. 1989: A simple tropical moist model applied to the '40 day' wave. *Quart. J. Roy. Meteor. Soc.*, to appear.

Davey, M.K. and G.R. Budin, 1989: Modelling Intraseasonal and Interannual variability in the tropics. *Phil. Trans. Roy. Soc.* , to appear.

Davey, M.K. and A.E. Gill, 1987: Experiments on tropical circulation with a moist model. *Quart. J. Roy. Meteor. Soc.*, 113, 1237-1270.

Gill, A.E., 1980: Some simple solutions for heat induced tropical circulation. *Quart. J. Roy. Meteor. Soc.*, 106, 447-462.

Gill, A.E., 1982a: Atmosphere - ocean dynamics. Academic Press, New York, International Geophysics Series, 30, pp662.

Gill, A.E., 1982b: Studies of moisture effects in simple atmospheric models: the stable case. *Geophys. Astrophys. Fluid Dynamics*, 19, 119-152.

Gill, A.E., 1982c: Spontaneously growing hurricane like disturbances in a simple baroclinic model with latent heat release. *Topics in atmospheric and oceanic sciences, Intense Atmospheric vortices* , eds. Bengtsson and Lighthill. Springer - Verlag, Berlin.

Gill, A.E., and P.J. Phlips, 1986: Nonlinear effects on heat-induced circulation of the tropical atmosphere. *Quart. J. Roy. Meteor. Soc.*, 112, 69-91.

Goldenburg, S.O., and J.J. O'Brien, 1981: Time and space variability of tropical Pacific wind stress. *Mon. Wea. Rev.*, 109, 1190-1207.

Greatbatch, R.J, 1985: Kelvin wave fronts, Rossby solitary waves and the nonlinear spin-up of the equatorial oceans. *J. Geophys. Res.*, 90, 9097-9107.

Haney, R.L., 1971: Surface thermal boundary condition for ocean circulation models. *J. Phys. Ocean.*, 1, 241-248.

Heckley, W.A. and A.E. Gill, 1983: Some simple analytical solutions to the problem of forced equatorial long waves. *Quart. J. Roy. Meteor. Soc.*, 110, 203-217.

Hirst, A.C., 1986: Unstable and damped equatorial modes in simple coupled ocean-atmosphere models. *J. Atmos. Sci.*, 43, 606-630.

Hirst, A.C., 1988: Slow instabilities in tropical ocean basin - global atmosphere models. *J. Atmos. Sci.*, 45, 830-852.

Holton, J.R., 1979: An introduction to dynamic meteorology. 2nd edn. Academic press, New York, 391pp.

Lau, K.-M. and P.H. Chan, 1988: Intraseasonal and interannual variations in tropical convection: A possible link between the 40 day mode and ENSO ?. Sub. to *J. Atmos. Sci.*

Lindzen, R.S., and S. Nigam, 1987: On the role of sea surface temperature gradients in forcing low-level winds and convergence in the tropics. *J. Atmos. Sci.*, 44, 2418-2436.

McCreary, J.P., 1985: Modeling equatorial ocean circulation. *Ann. Rev. Fluid Mech.*, 17, 359-409.

Matsuno, T., 1966: Quasi geostrophic motions in the equatorial area. *J. Meteor. Soc. Japan*, 44, 25-43.

Oort, A.H., 1983: Global atmospheric circulation statistics 1958-1973.NOAA professional paper No. 14, U.S. Dept. of Commerce, National Oceanic and Atmospheric Administration, pp180.

Sardeshmukh, P.D. and B.J. Hoskins, 1985: Vorticity balances in the tropics during the 1982-83 El niño- Southern Oscillation event. *Quart. J. Roy. Meteor. Soc.*, 111, 261-278.

Shea, D.J., 1986: Climatological Atlas 1950-1979. Surface air temperature, precipitation, sea-level pressure and sea-surface temperature (45 °S - 90 °N). NCAR Technical Note TN-269 ,NCAR ,Boulder.

Swinbank, R., T.N. Palmer, and M.K. Davey, 1988: Numerical simulations of the Madden and Julian oscillation. *J. Atmos. Sci.*, 45, 774-788.

Weare, B.C., 1986a: A simple model of the tropical atmosphere driven by a circulation - dependent forcing. *Quart. J. Roy. Meteor. Soc.*, 112, 409-429.

Weare, B.C., 1986b: A simple model of the tropical atmosphere with circulation - dependent heating and specific humidity. *J. Atmos. Sci.*, 43, 2001-2016.

Weare, B.C., P.T. Strub, and M.D. Samuel, 1980: Marine climate atlas of the tropical Pacific ocean. *Contributions to Atmospheric Sciences*, No. 20, University of California at Davis, USA, 147pp.

Webster, P.J., 1972: Response of the tropical atmosphere to local steady forcing. *Mon. Wea. Rev.*, 100, 518-541.

Webster, P.J., 1982: Seasonality in the local and remote atmospheric response to sea surface temperature anomalies. *J. Atmos. Sci.*, 39, 41-52.

Wells, N.C. and S. King-Hele, 1989: Parameterisation of tropical ocean heat flux. Sub. to *Quart. J. Roy. Meteor. Soc.*

Yamagata, T., 1987: On the recent development of simple, coupled ocean - atmosphere models of ENSO. *J. Ocean. Soc. Japan*, 42, 299-307.

Yamagata, T., and Y. Masumoto, 1989: A simple ocean-atmosphere model of the origin of a warm ENSO event. Subj. to *J. Meteor. Soc. Japan*

Yanai,M., S. Esbensen and J.H. Chu, 1973: Determination of bulk properties of tropical cloud clusters from large scale heat and moisture budgets. *J. Atmos. Sci.*, 30, 611.

Zebiak, S.E., 1982: A simple atmospheric model of relevance to El niño. *J. Atmos. Sci.*, 39, 2017-2027.

Zebiak, S.E., 1986: Atmospheric convergence feedback in a simple model for El niño. Sub. to *Mon. Wea. Rev.*, 114, 1263-1271.

**Table 1a. Typical atmospheric model input parameter list.**

| Symbol in text | Value | Units | Value | Units* |
|---|---|---|---|---|
| Maximum latitude of grid | 30 | ° | | |
| Width of grid | 144 | ° | | |
| $\delta t_a$ | 1200 | *secs* | 20 | *mins* |
| H | 5410 | m | $17/\pi$ | km |
| $\frac{d\theta_0}{dz}$ | 3.9E-03 | $°/m$ | | |
| $\theta_{00}$ | 310 | K | | |
| $Q_f$ | 6.8E-02 | m | | |
| $RH_c$ | 0.8 | | | |
| $E_v$ | 4.E-07 | $m^{-1}$ | | |
| $E_0$ | 1.E-06 | $sec^{-1}$ | 1/7 | $days^{-1}$ |
| $lt^+_{eq}$ | 29.5 | $°C$ | | |
| $lt^+_{bn}$ | 23.5 | $°C$ | | |
| $SM^+_d$ | 1.5E-02 | $m$ | 15 | cm |
| $T^{ref}_s$ | 26.5 | $°C$ | | |
| $\nu$ | 1.0E05 | $m^2 sec^{-1}$ | | |
| $\eta$ | 5.0E-06 | $sec^{-1}$ | 1/3 | $days^{-1}$ |

* Second value and units columns are just to show some values in figures more easily interpreted.

+ These parameters are only needed when including land processes in the model.

**Table 1b. Physical constants for the atmospheric model.**

| Name | Description | Value | Units |
|---|---|---|---|
| $\beta$ | Latitudinal gradient of f | 2.28E-11 | $m/sec$ |
| $\rho_{oo}$ | Reference atmospheric density | 1.225 | $kgm^{-3}$ |
| $L$ | Latent heat of vaporization | 2.5E06 | $JKg^{-1}$ |
| $C_p$ | Specific heat of air | 1004 | $JKg^{-1}\ ^{\circ}C$ |

**Table 1c. Dependent atmospheric model parameters.**

| Name | Description | Value | Units |
|---|---|---|---|
| $m$ | Moisture factor | 234.7 | $^{\circ}C/m$ |
| $N$ | Buoyancy frequency | 1.11E-02 | $secs^{-1}$ |
| $a$ | Rossby radius | 1.15E06 | $m$ |
| $c$ | Gravity wave speed | 57.0 | $m/sec$ |
| $\tau$ | Time scale | 1.9E04 | $secs$ |

**Table 2a. Ocean model parameters**

| Name in text | Description | Value | Units |
|---|---|---|---|
| $w$ | Background upwelling | 4.E-07 | $m/sec$ |
| $\delta_o$ | wind mixing parameter | 2.74E-02 | $m^3{}^\circ C/sec$ |
| $\gamma$ | Haney heat flux coefficient | 3.E-06 | $m/sec$ |
| $\nu$ | Ocean viscosity | 2.E04 | $m^2/sec$ |

**Table 2b. Physical constants for the ocean model.**

| Name | Description | Value | Units |
|---|---|---|---|
| $\rho_w$ | Water density | 1.E03 | $kg/m^3$ |
| $\alpha$ | Water thermal expansion coefficient | 2.E-04 | $^\circ C^{-1}$ |
| $\rho_a$ | Atmospheric surface density | 1.2 | $kg/m^3$ |

**Table 2c. Ocean model dependent parameters**

| Name | Description | Value | Units |
|---|---|---|---|
| $N$ | Buoyancy frequency | 2.4E-02 | $secs^{-1}$ |
| $a$ | Rossby radius | 2.3E05 | $m$ |
| $c$ | Gravity wave speed | 1.4 | $m/sec$ |

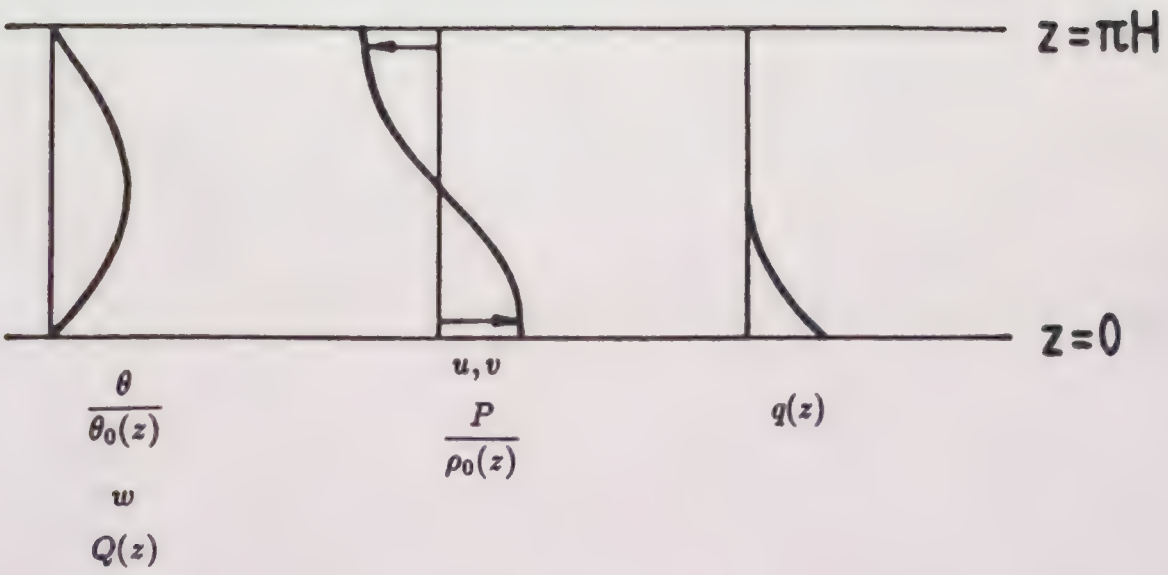


Fig. 1. The vertical structure assumed in the atmospheric model. Potential temperature perturbation (divided by a reference vertical potential temperature profile $\theta_0(z)$), $\frac{\theta}{\theta_0(z)}$ , vertical velocity, $w$, and heating, $Q$ (given by: $Q = Q_l + Q_f$ with $Q_l$ the latent heating and $Q_f$ a fixed heating) , are largest at the mid-tropospheric level. Horizontal velocity $(u, v)$ , and pressure perturbation (divided by a reference vertical density profile $\rho_0(z)$), $\frac{P}{\rho_0(z)}$ have largest and opposite values at lower and upper levels. Moisture, $q$, is confined to low levels. Davey and Gill (1988) give details of the reduction of full model (three dimensional) equations to horizontal ones using the above vertical profiles.

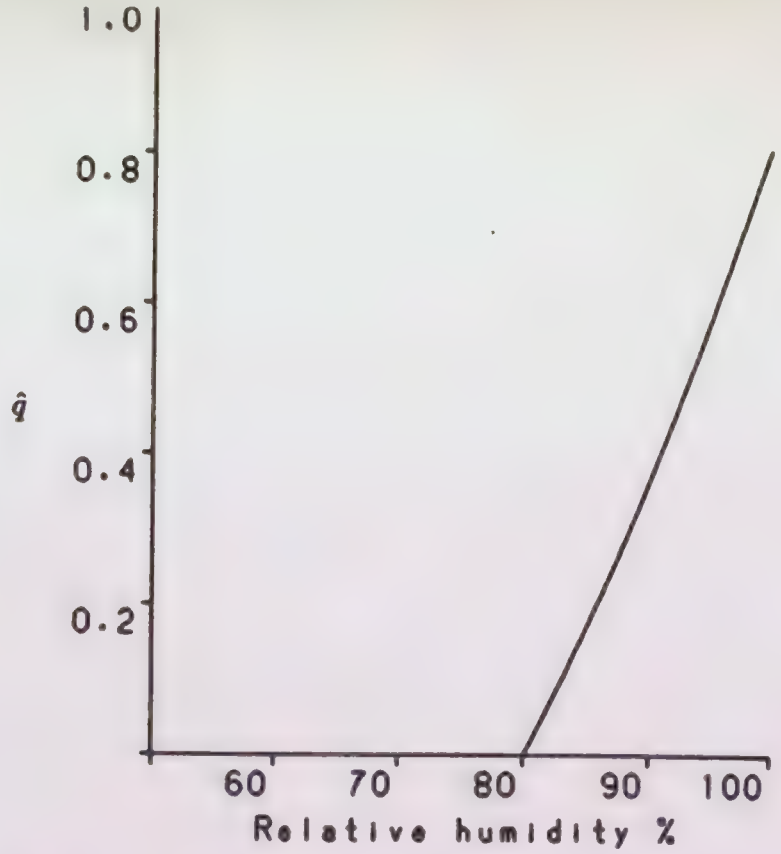


Fig. 2a. Variation of $\hat{q}$ with relative humidity, for a temperature of 28 °C and critical relative humidity, $RH_c = 0.80$.

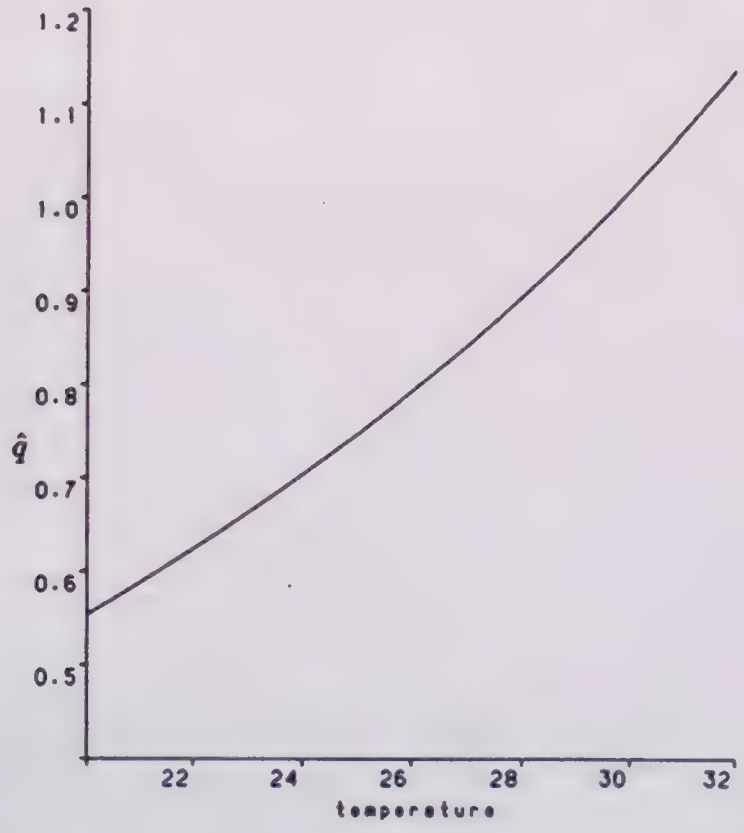


Fig. 2b. Variation of $\hat{q}$ with temperature at saturation.

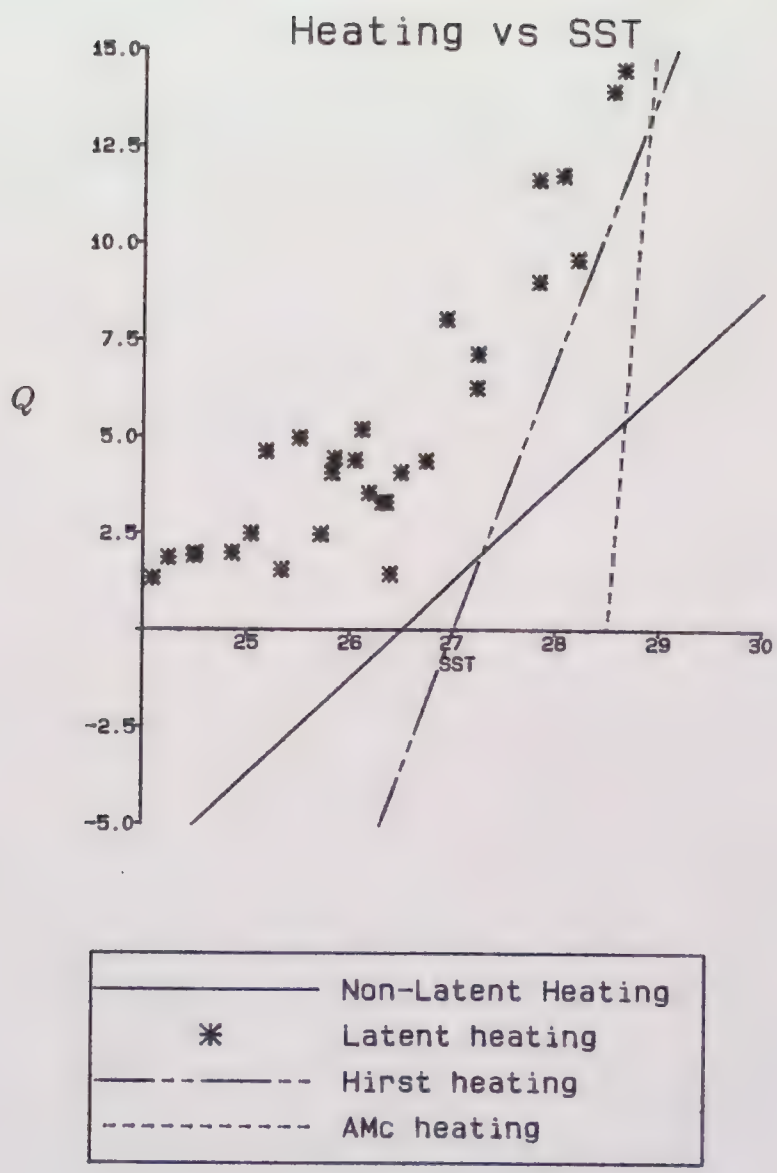


Fig 3. Mid-level heating as a function of surface temperature for the present model: non-latent heating (solid-line), latent heating (starred points), and for the heating profile used by Hirst (1986) and (1988) (dot-dashed line) and Anderson and McCreary (1985a) (dotted line). Heating has been scaled to be in the units used by Anderson and McCreary, $m^2/s^3$.

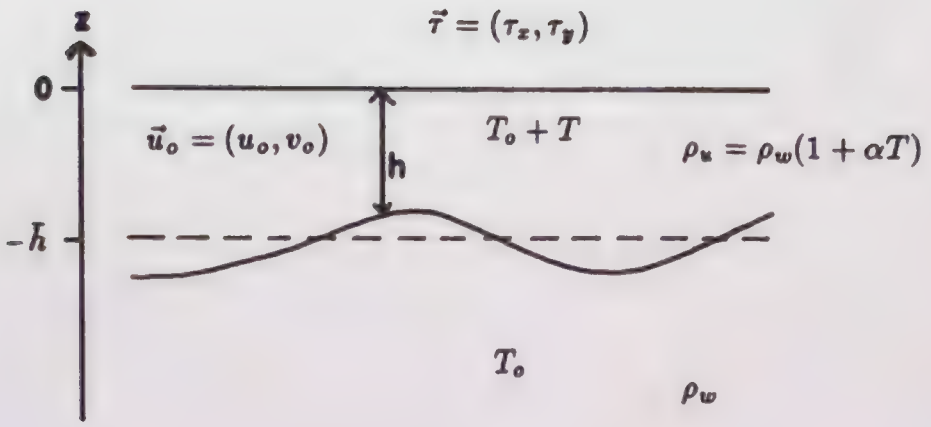


Fig. 4. The one-active layer ocean model, vertical cross-section. $\bar{h}$ is the mean thermocline depth, h, the varying depth. T is the temperature excess of the active layer over the motionless, inert lower layer at temperature $T_0$. The lower layer has constant density $\rho_w$, the upper layer density $\rho_u$ varies with temperature as indicated. $\tau$ is the surface wind stress, $\vec{u}_o$ the currents.

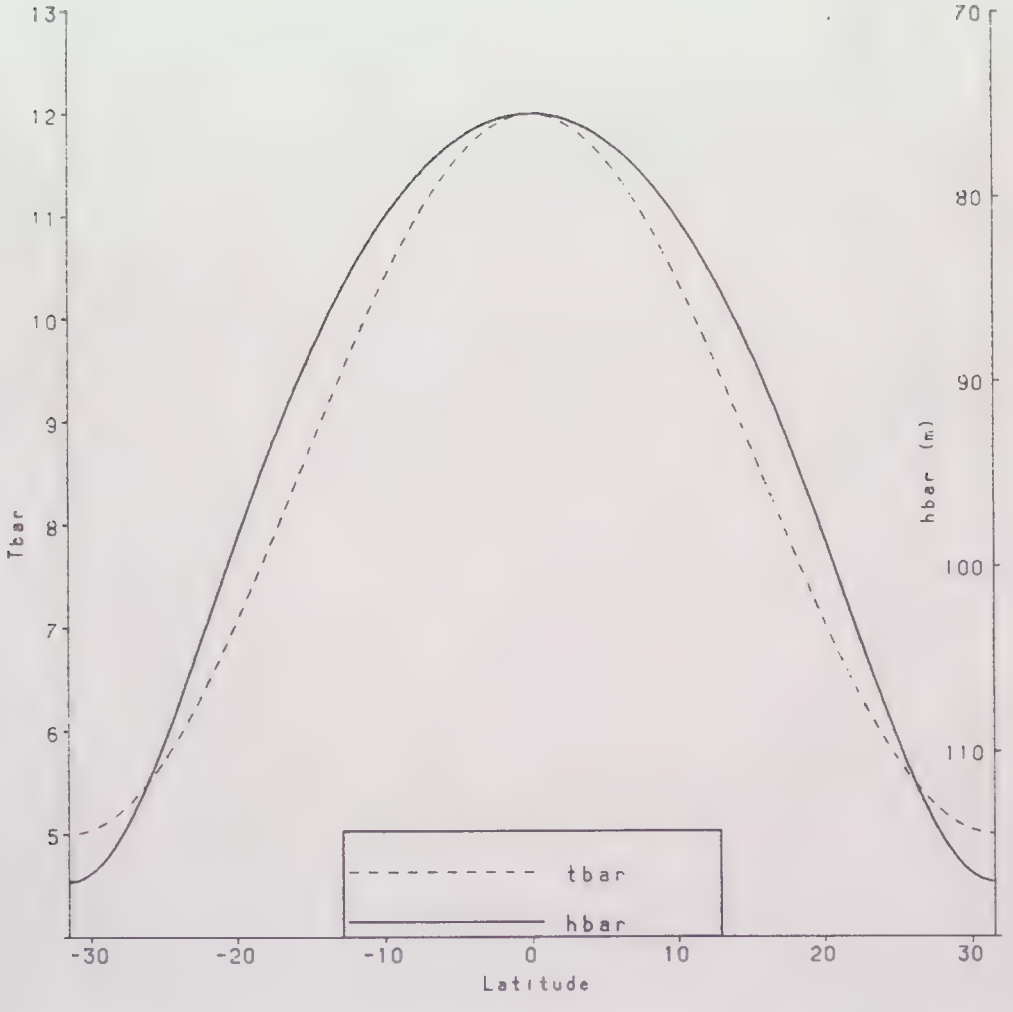


Fig. 5. Variation of $\bar{T}$ and $\bar{h}$ with latitude for the ocean model parameters as in Table 2. Sea surface temperature is $\bar{T}+T_0$, with the deep ocean temperature $T_0 = 17°C$.

Fig. 6. Atmospheric model Arakawa C-grid. Surface pressure $P$ and moisture $q$ are defined at the $\theta$ points, the wind components $u$ and $v$ are half a grid point away in the $x$ and $y$ directions, respectively.

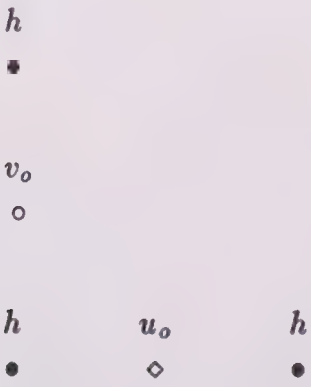


Fig. 7. Ocean model Arakawa C-grid. SST is defined at the $h$ points, the current components $u_o$ and $v_o$ are half a grid point away in the $x$ and $y$ directions, respectively.

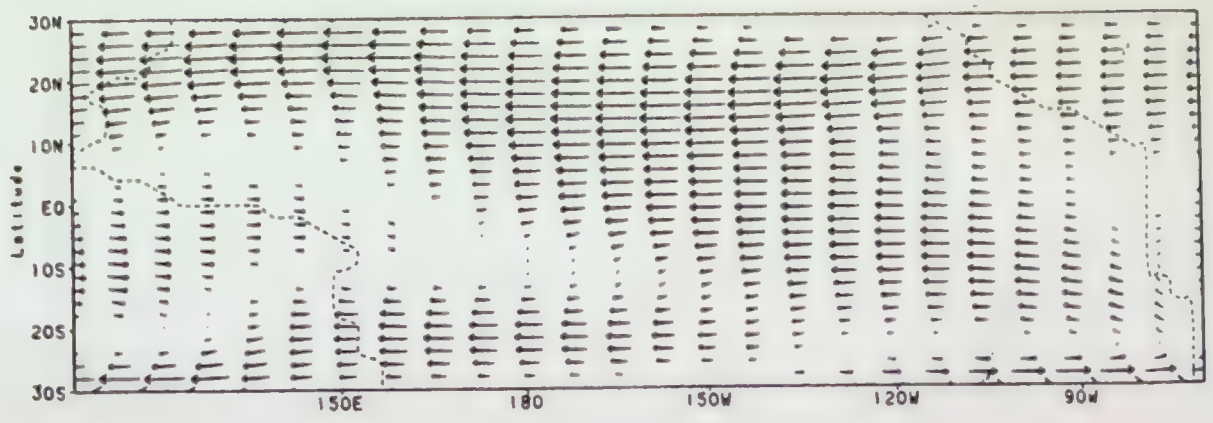


Fig 8a. Atmospheric low level wind field ($m/sec$) averaged for January when forced with climatological SST's. The land-ocean boundary is drawn as a dotted line. The maximum wind is 10.3 $m/sec$, and vectors with speed less than 0.1 times this maximum are not drawn.

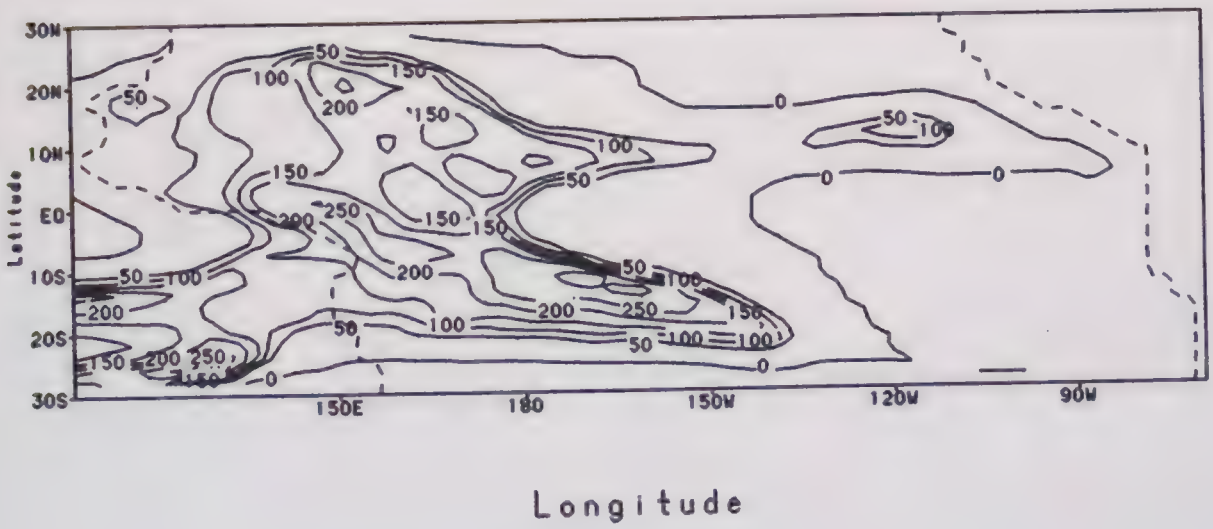


Fig. 8b. As in 8a. but precipitation in *mm/month* with a maximum value of 320 *mm/month*.

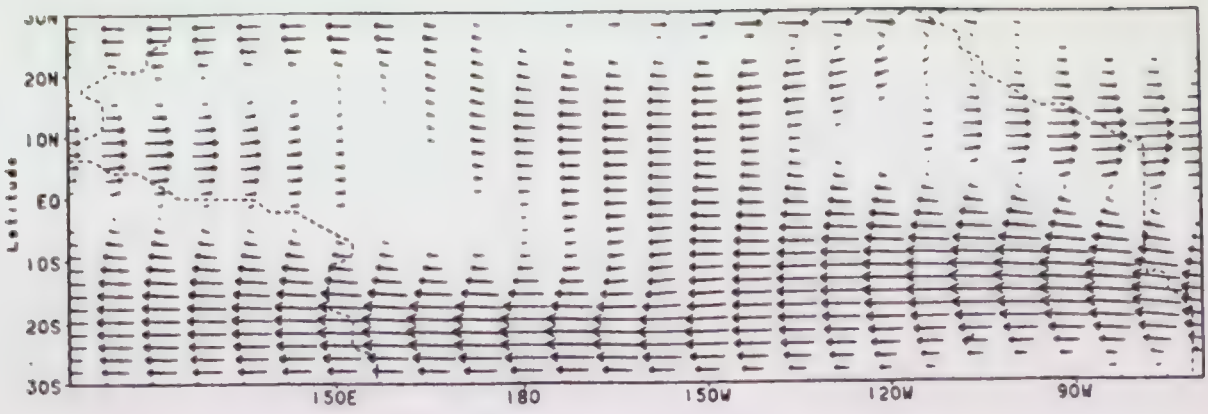


Fig 9a. Atmospheric low level wind field ($m/sec$) averaged for July when forced with climatological SST's. The land-ocean boundary is drawn as a dotted line. The maximum wind is 10.1 $m/sec$, and vectors with speed less than 0.1 times this maximum are not drawn.

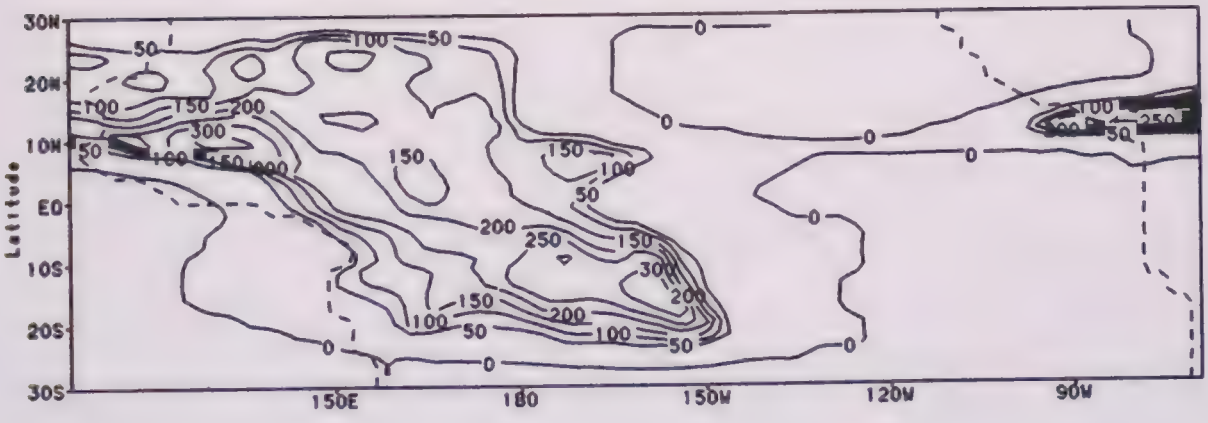


Fig. 9b. As in 9a. but precipitation in $mm/month$ with a maximum value of 320 $mm/month$.

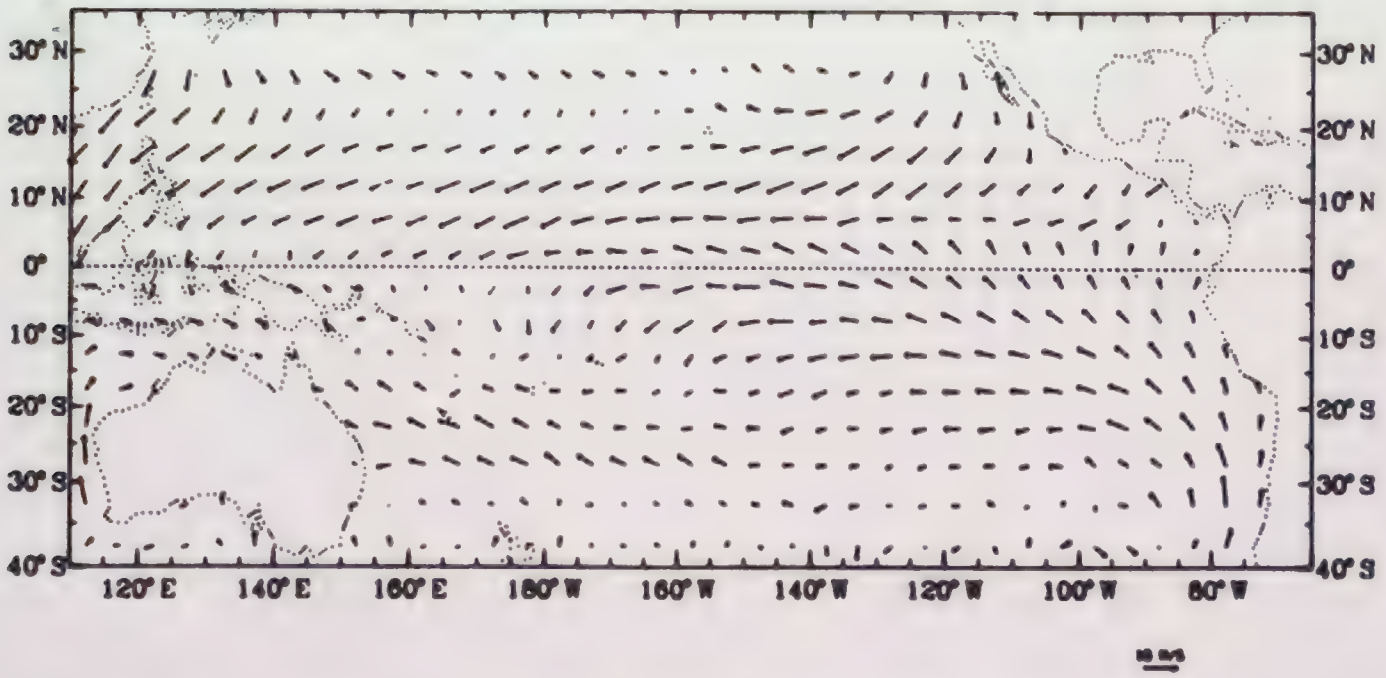


Fig. 10a. Climatological atmospheric surface wind field $m/sec$ for January (after Weare, Strub and Samuel, 1980). A reference vector of 10 $m/sec$ in indicated.

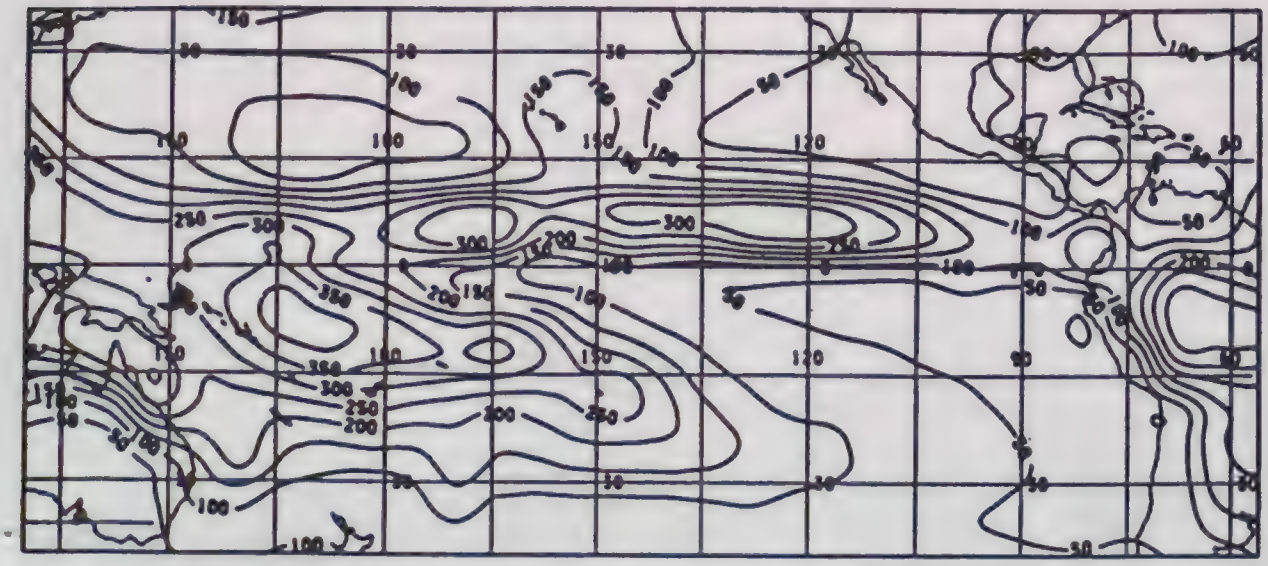

Fig. 10b. January climatological precipitation ($mm/month$) (after Shea, 1986) .

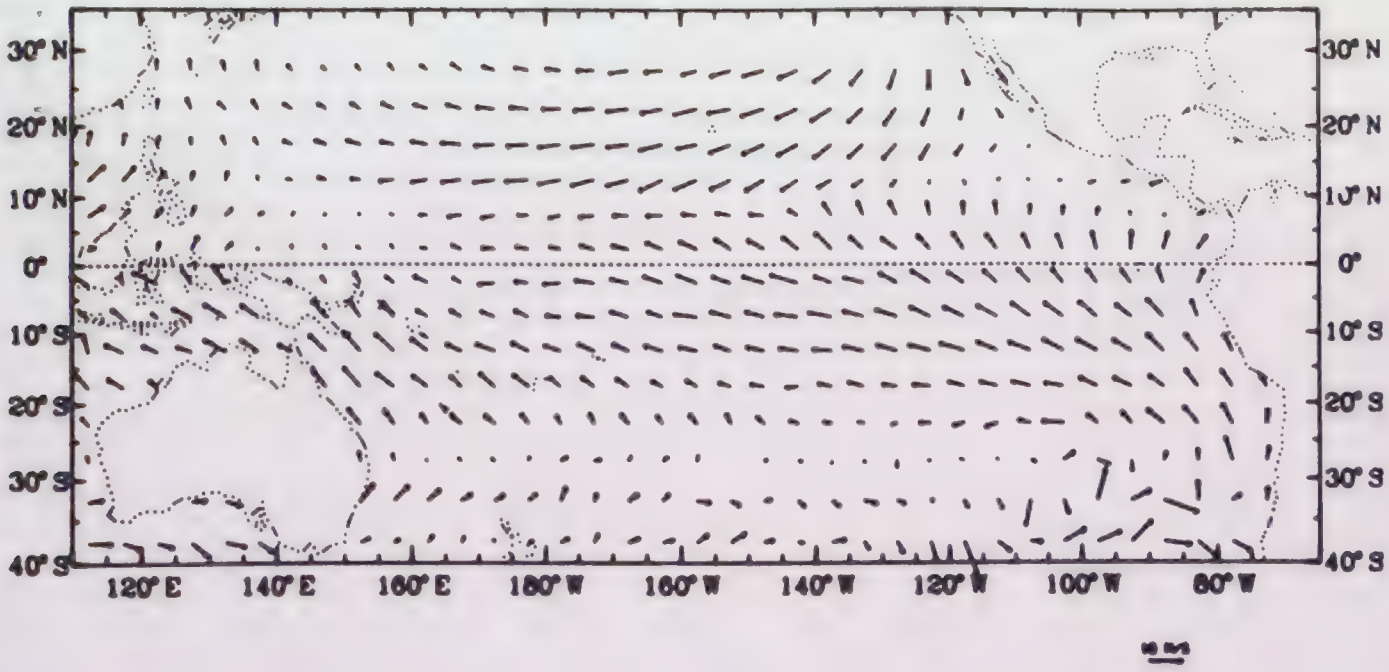


Fig. 11a. Climatological atmospheric surface wind field *m/sec* for July (after Weare, Strub and Samuel, 1980). A reference vector of 10 *m/sec* in indicated.

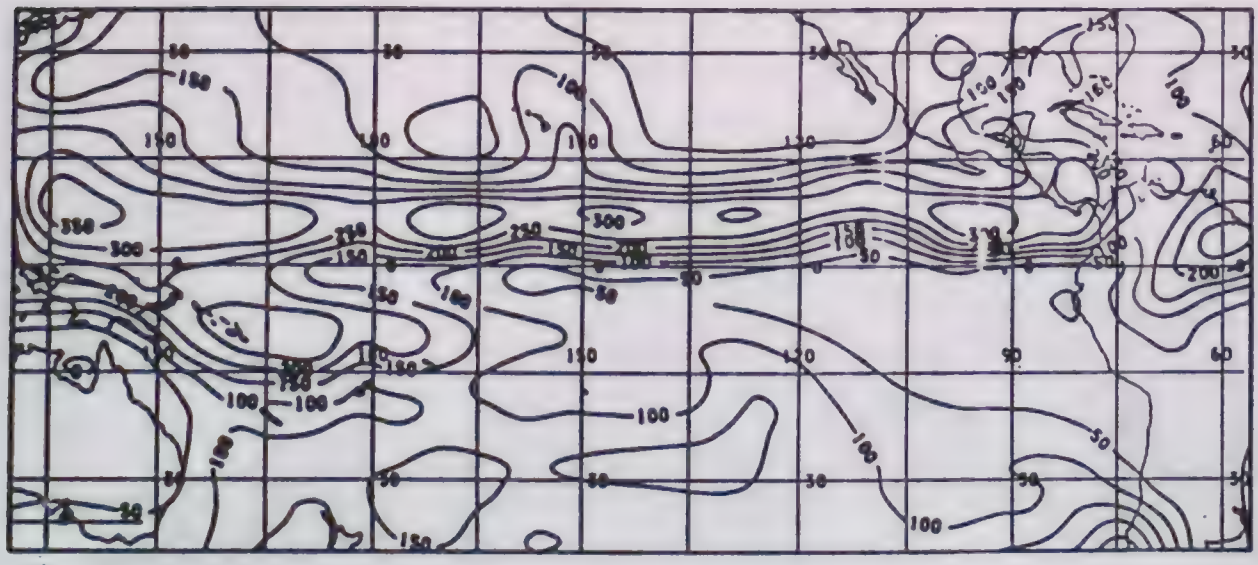

Fig. 11b. July climatological precipitation (*mm/month*) (after Shea, 1986) .

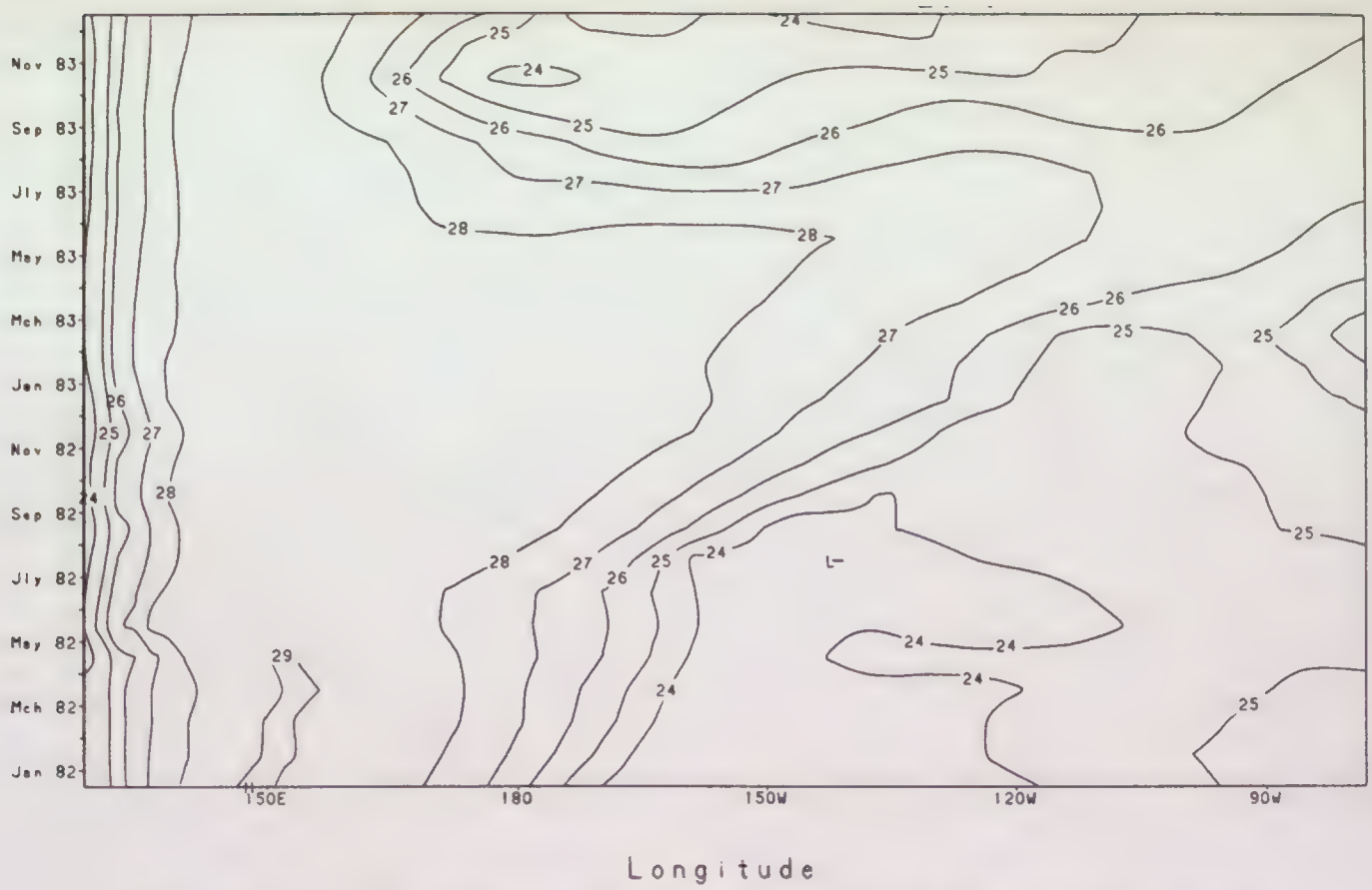


Fig. 12a. SST (°C) along 1°N for ocean model forced with observed winds for 1982/83. Minimum = 23.0, maximum = 29.0

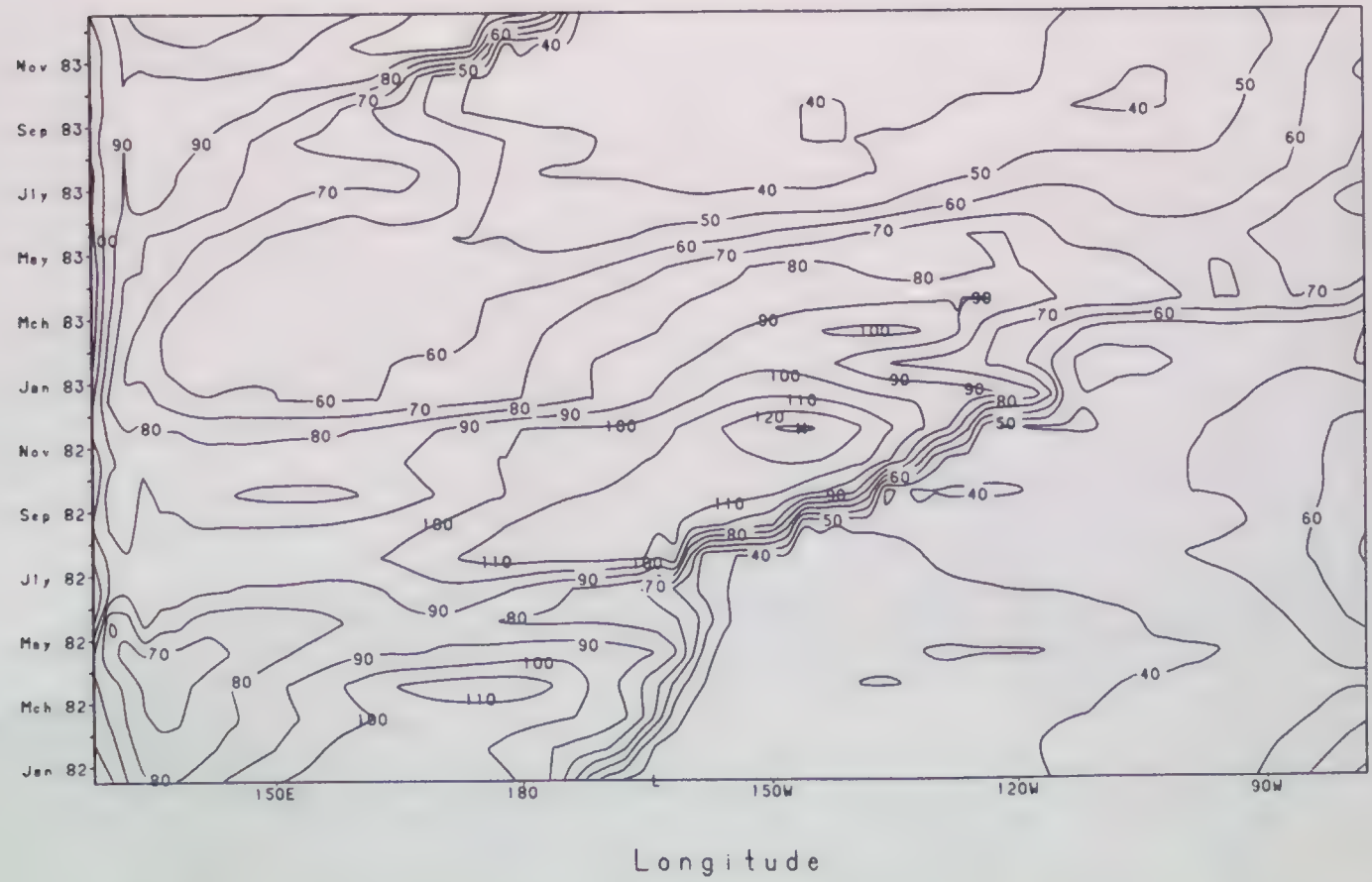


Fig. 12 b. As in a. but thermocline depth (m): minimum = 35, maximum = 131.

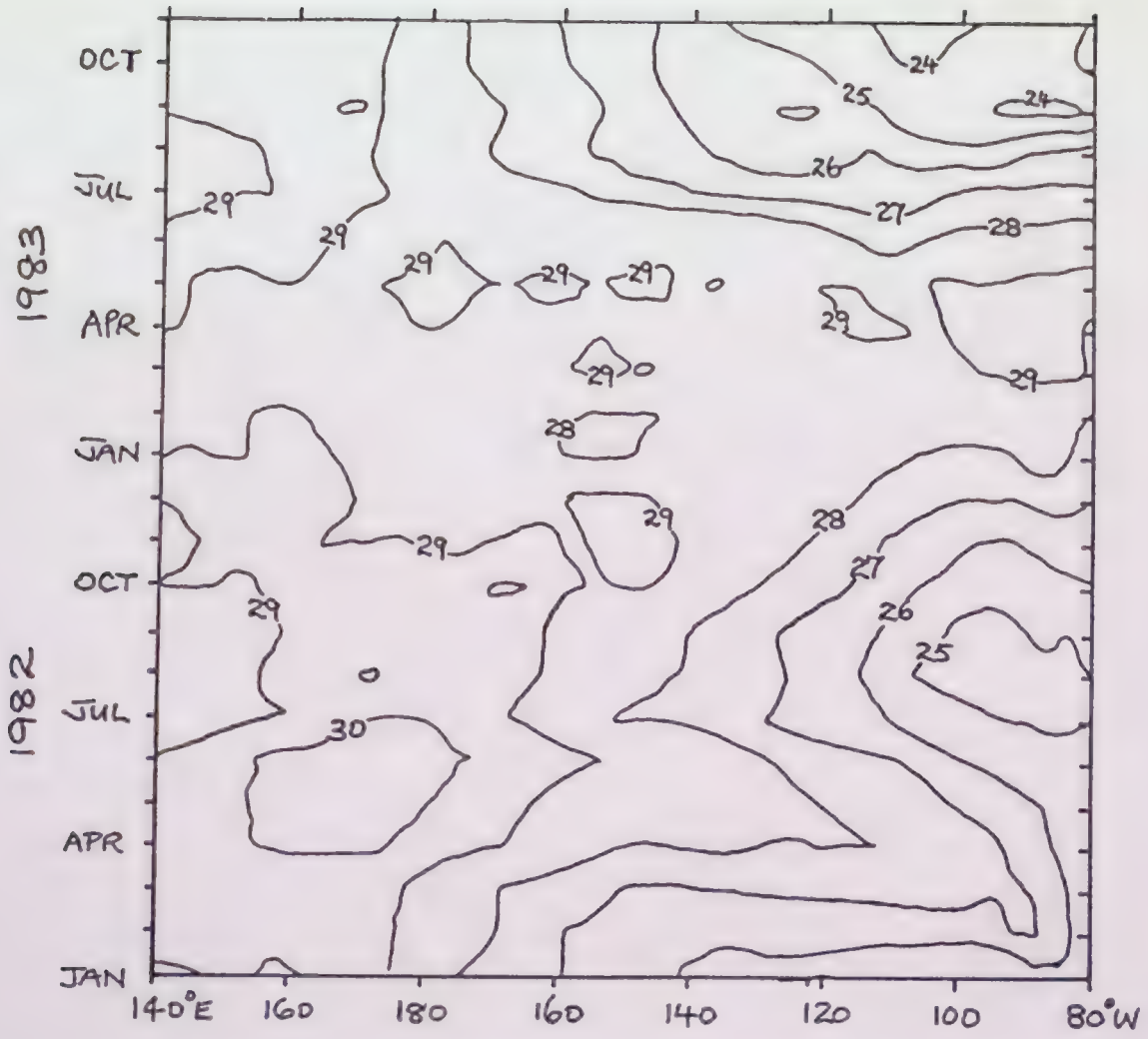


Fig. 13. Observed SST (°C) along the equator during 1982/83 (after Reynolds, private communication).

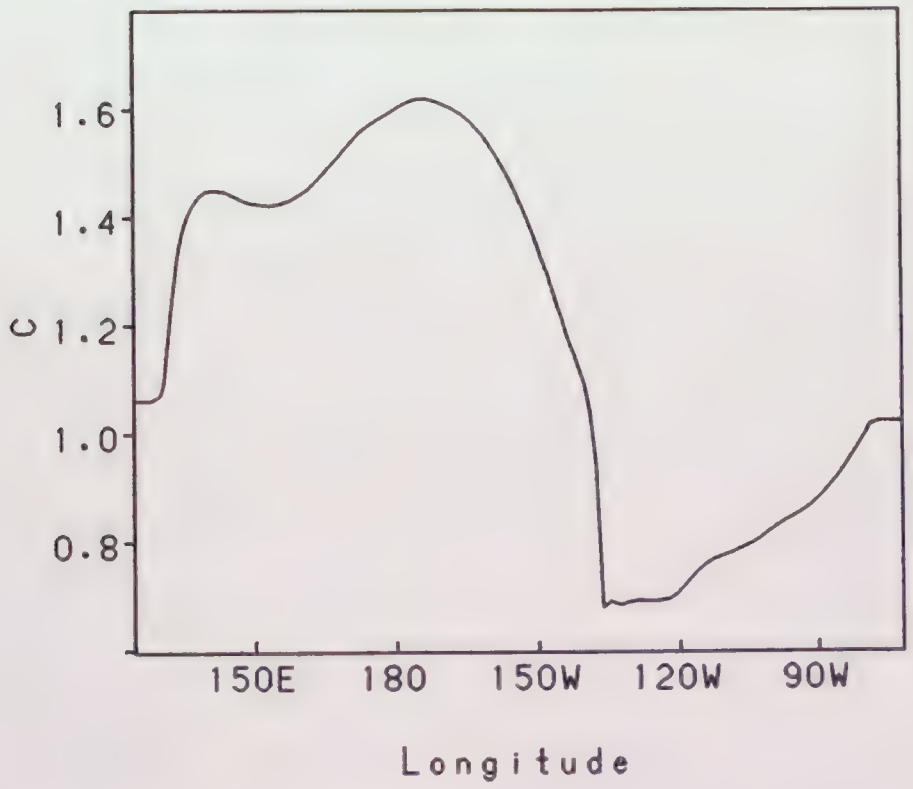


Fig. 14. Ocean model gravity wave speed (m/sec) along 1 °N for September, 1982.

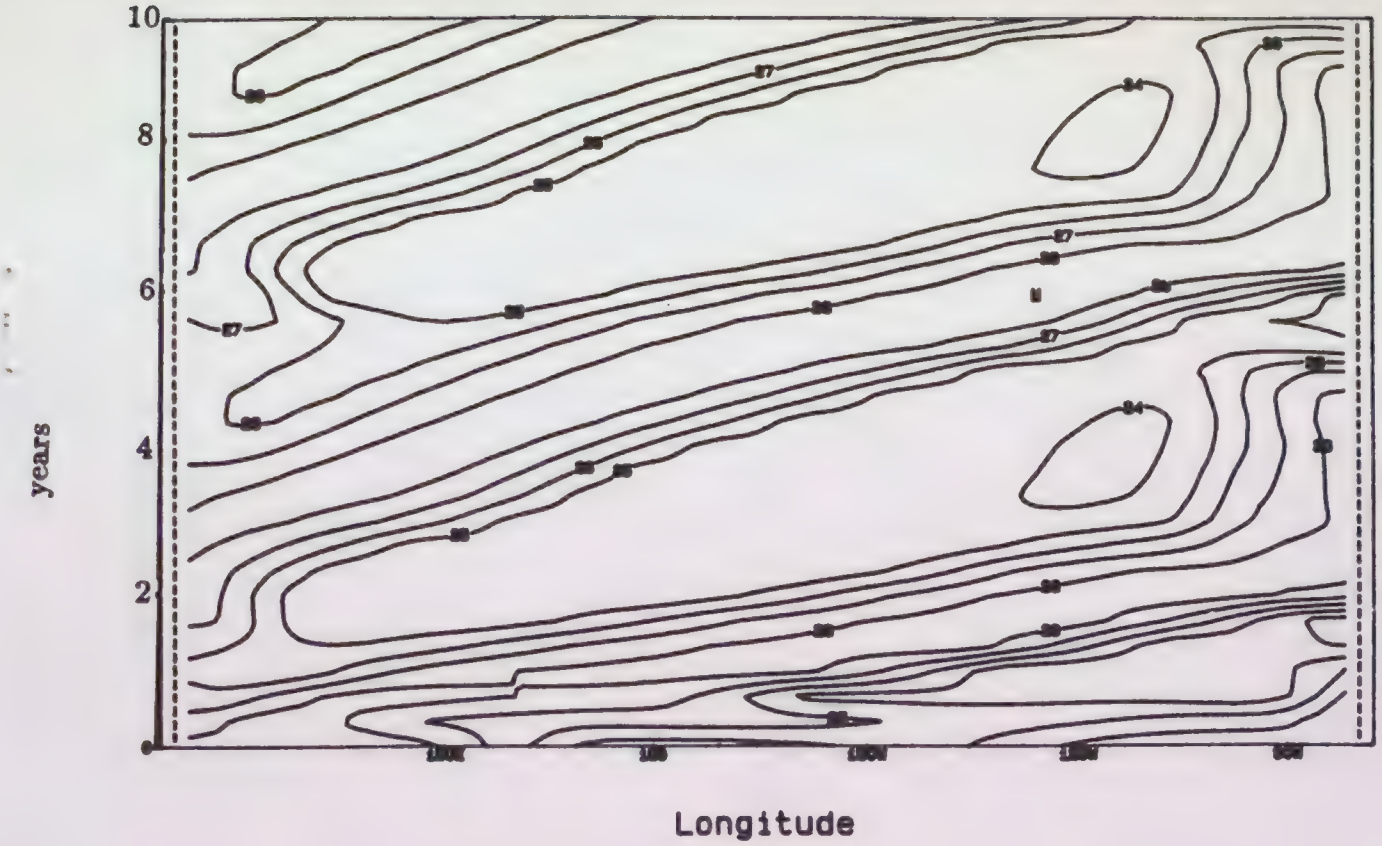


Fig. 15a. SST (°C) along 2 °N for a coupled model the width of the Pacific. Minimum = 23.7, maximum = 28.8.

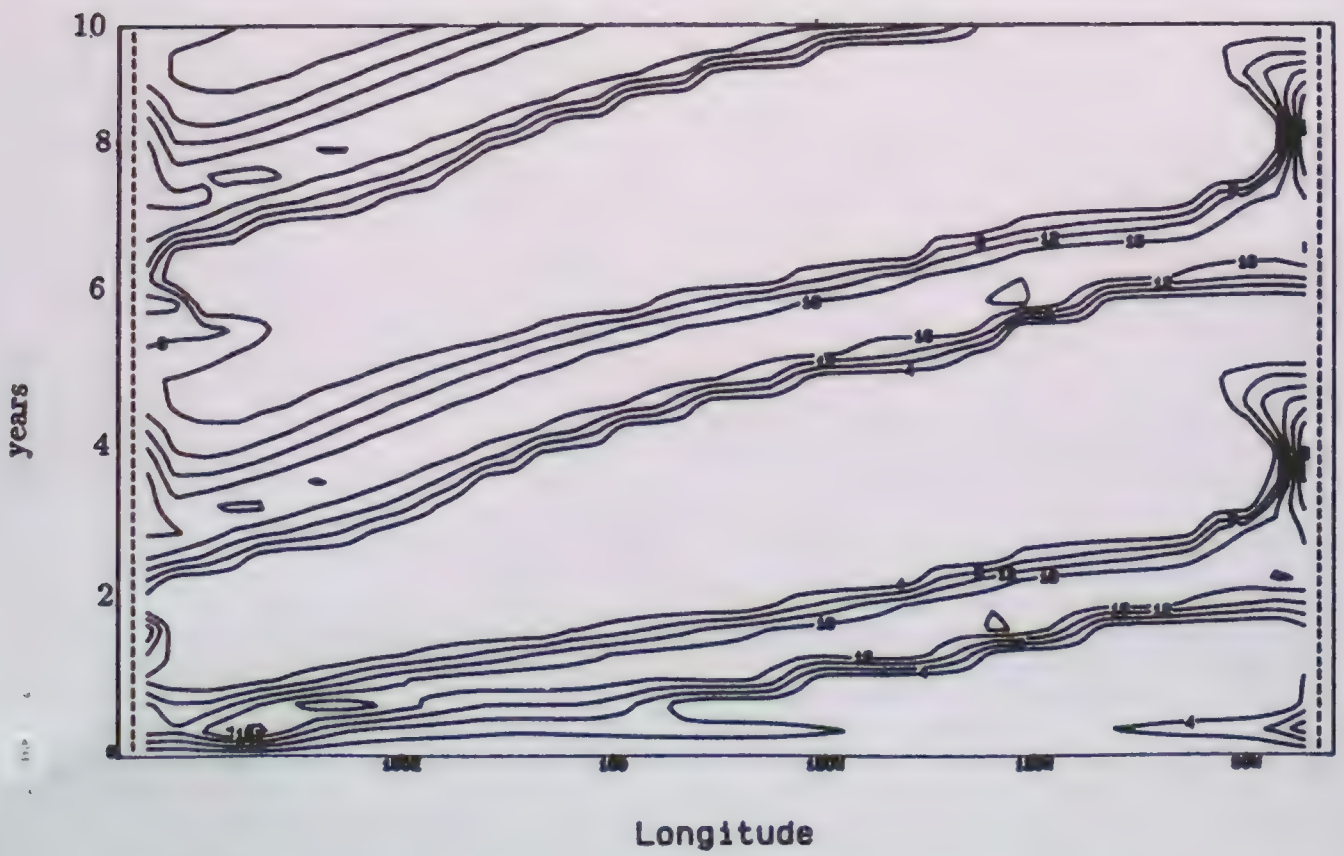


Fig. 15b. As in a. but precipitation (mm/day): maximum = 28.8.

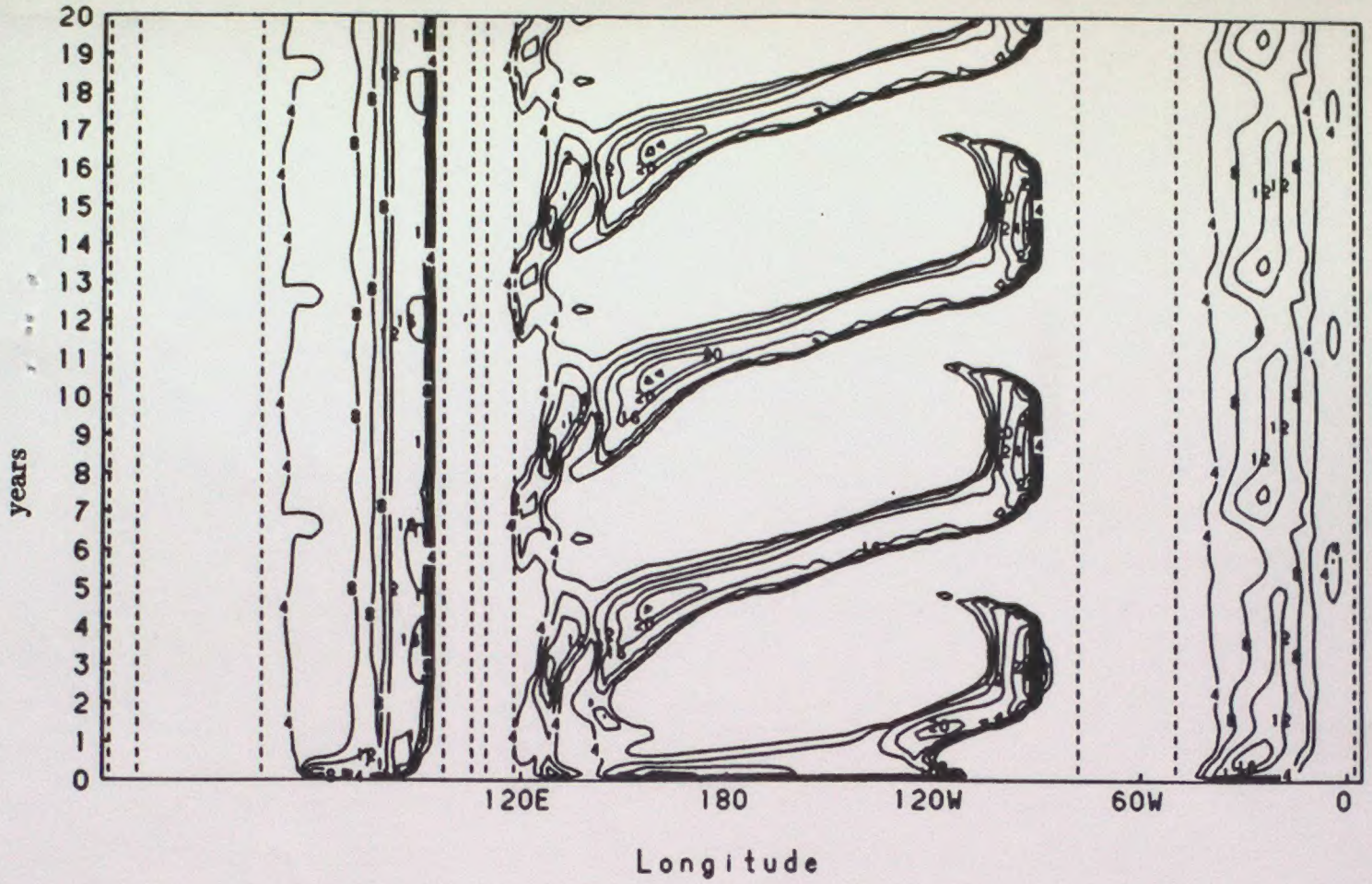


Fig. 16. Precipitation (mm/day) along 2 °N for a 20 year experiment using the coupled model with world geometry. Maximum = 30.4. Dashed line indicates land/ocean boundary.

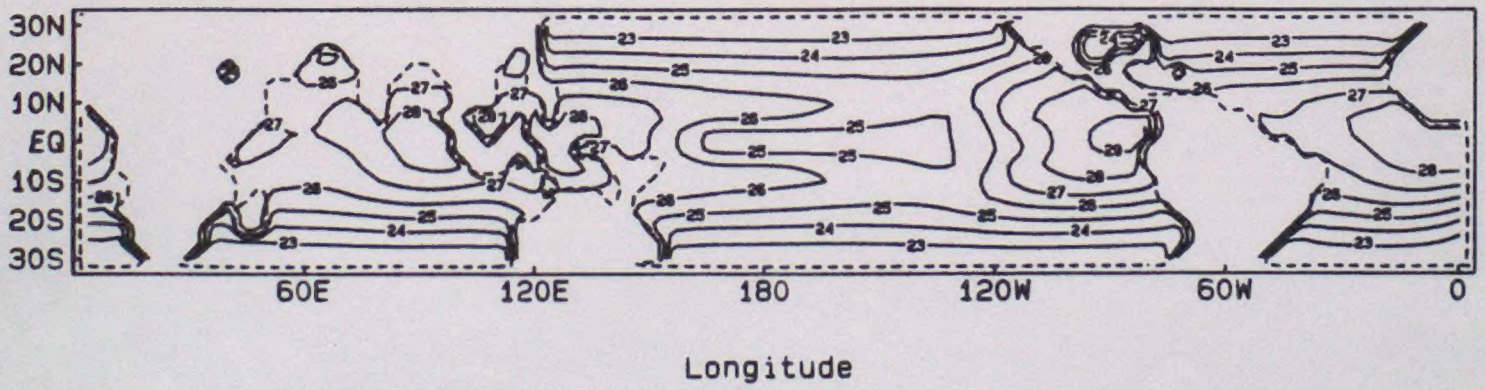


Fig. 17. Surface temperature (°C) at the end of 20 years for coupled model with world geometry. Minimum = 22.1, maximum = 29.3.

DYNAMICAL CLIMATOLOGY TECHNICAL NOTES

| | | |
|---|---|---|
| DCTN 1 | June 1984 | A scheme for incorporating the thermodynamic sea-ice model into a coupled ocean-atmosphere model.<br>C Gordon and M Bottomley |
| DCTN 2 | Sept 1984 | The parametrization of the upper ocean mixed layer in coupled ocean/atmosphere models.<br>C Gordon and M Bottomley |
| DCTN 3 | Sept 1984 | The response of a simple thermodynamic sea-ice model to GCM forcing appropriate for perennial sea-ice.<br>M Bottomley |
| DCTN 4 | Sept 1984 | Potential vorticity in the stratosphere derived using data from satellites.<br>S A Clough, N S Grahame and A O'Neill |
| DCTN 5 | Sept 1984 | Simulation of the seasonal cycle of SST using globally specified climatological data to force simple ocean models.<br>N S Grahame |
| DCTN 6 | Sept 1984 | Development of an improved GCM radiation scheme.<br>A Slingo and R C Wilderspin |
| DCTN 7 | Sept 1984 | On the specification of surface fluxes in coupled atmosphere/ocean general circulation models.<br>J F B Mitchell, C A Wilson and C M Price |
| DCTN 8 | Sept 1984 | A survey of possible repercussions of the Soviet river reversal programme on Arctic sea-ice.<br>H Cattle |
| DCTN 9 | Oct 1984 | A study of a strong stratospheric warming during January 1982<br>T D A Fairlie |
| DCTN 10 | Nov 1984 | An intercomparison of the Met O 11 N45 model and the Met O 20 11-level model on the Cyber 205<br>J F Dyson |
| DCTN 11 | Nov 1984 | Simulation of observed time series of temperature and precipitation over eastern England.<br>D N Reed |
| DCTN 12 | Nov 1984 | Forecasts and analyses of the onset of the Southwest monsoon.<br>R Kershaw |
| DCTN 13 | Nov 1984 | On modelling the effects of $CO_2$ on climate.<br>J F B Mitchell |
| DCTN 14 | Dec 1984 | Development of a revised longwave radiation scheme for an atmospheric general circulation model.<br>A Slingo and R C Wilderspin |
| DCTN 15 | Jan 1985 | Rossby wavetrains in the stratosphere forced by localised disturbances in the troposphere.<br>C J Marks (Oxford), A O'Neill and V D Pope |

DYNAMICAL CLIMATOLOGY TECHNICAL NOTES

| | | |
|---|---|---|
| DCTN 16 | Jan 1985 | Observing system experiments using the Meteorological Office's 15-level model.<br>R A Bromley |
| DCTN 17 | Feb 1985 | Atmospheric general circulation simulation of the climate of the Mediterranean region.<br>H Cattle |
| DCTN 18 | Feb 1985 | Diurnal variation and cloud in a general circulation model.<br>C A Wilson and J F B Mitchell |
| DCTN 19 | Feb 1985 | The sensitivity of the Saharan region in a general circulation model.<br>W M Cunnington and P R Rowntree |
| DCTN 20 | Mar 1985 | The impact of aircraft observations on analyses and forecasts from the operational 15-level model.<br>B R Barwell |
| DCTN 21 | Mar 1985 | Non-linear effects on heat-induced circulation of the tropical atmosphere.<br>A E Gill and P J Phlips |
| DCTN 22 | Apr 1985 | Simulation of cloudiness with the U.K. Meteorological Office 11-layer AGCM.<br>A Slingo and R C Wilderspin |
| DCTN 23 | Apr 1985 | An integrated approach to the representation of cloud processes. R N B Smith |
| DCTN 24 | May 1985 | Nuclear Winter: Calculations of the shortwave radiative effects of soot aerosols.<br>A Slingo and P Goldsmith |
| DCTN 25 | Jul 1985 | Sea ice and the Antarctic winter circulation: a numerical experiment.<br>J F B Mitchell and T S Hills |
| DCTN 26 | Jul 1985 | A Budyko-Sellers model for study of ocean-atmosphere interaction.<br>W J Ingram |
| DCTN 27 | Aug 1985 | The effect of a shoaling thermocline on equatorially-trapped Kelvin waves.<br>A E Gill and B A King |
| DCTN 28 | Sept 1985 | $CO_2$ climate sensitivity and model dependence of results.<br>J F B Mitchell, C A Wilson and W M Cunnington |
| DCTN 29 | Sept 1985 | Handbook of the Meteorological Office 11-layer atmospheric general circulation model.<br>Volume 1 : Model Description<br>Edited by A Slingo |
| DCTN 30 | Sept 1985 | Impact of land surface variations on African rainfall in general circualation models.<br>P R Rowntree, M F Wilson and A B Sangster |

DYNAMICAL CLIMATOLOGY TECHNICAL NOTES

DCTN 31 Nov 1985 The annual cycle of sea level in the eastern tropical Pacific.
G R Bigg and A E Gill

DCTN 32 Nov 1985 An analytic model of the heat-induced tropical circulation in the presence of a mean wind.
P J Phlips and A E Gill

DCTN 33 Nov 1985 The effect of resolution and diffusion on the simulated climate.
J F Dyson

DCTN 34 Jan 1986 Rossby adjustment over a step.
M K Davey, A E Gill, E R Johnson and P F Linden

DCTN 35 Jan 1986 Issues concerning the evaluation of effective surface roughness of heterogeneous terrain.
D J Carson

DCTN 36 Mar 1986 Climate sensitivity and past climates : evidence from numerical studies
J F B Mitchell

DCTN 37 Mar 1986 Parametrizations of land-surface processes in Meteorological Office numerical weather prediction and climate models
D J Carson

DCTN 38 Apr 1986 Modelling of land-surface processes and their influence on European Climate
D A Warrilow, A B Sangster and A Slingo

DCTN 39 Apr 1986 Simulation of climatic change due to increased $CO_2$
J F B Mitchell

DCTN 40 May 1986 On the interpretation of the Eliassen-Palm flux divergence. Part I : Theory
D G Andrews

DCTN 41 June 1986 Experiments on tropical circulation with a simple moist model.
M K Davey and A E Gill

DCTN 42 Jun 1986 Parameter regimes for studying isolated eddies.
P D Killworth and M K Davey

DCTN 43 Jun 1986 A comparison of the impact of an envelope orography and of a parametrization of orographic gravity-wave drag on model simulations.
A Slingo and D W Pearson

DCTN 44 Jul 1986 The effect of a sea-surface temperature anomaly on a prediction of the onset of the south-west monsoon over India.
R Kershaw

DCTN 45 Jul 1986 An introduction to the parametrization of land-surface processes.
D J Carson

DYNAMICAL CLIMATOLOGY TECHNICAL NOTES

DCTN 46 Sept 1986 Lateral boundaries and the heat-induced flow in the tropical atmosphere.
P J Phlips and A E Gill

DCTN 47 Nov 1986 Simulation of the diurnal cycle of outgoing longwave radiation with an atmospheric GCM.
A Slingo, R C Wilderspin and S J Brentnall

DCTN 48 Feb 1987 A 2 x $CO_2$ climate sensitivity experiment with a global climate model including a simple ocean
C A Wilson and J F B Mitchell

DCTN 49 Feb 1987 Sensitivity of the Met O 20 11-layer model to increased land surface roughness length
C C Heasman

DCTN 50 Feb 1987 The influence of atmospheric waves on the general circulation of the middle atmosphere
D G Andrews

DCTN 51 Feb 1987 Transport mechanisms in the middle atmosphere: an introductory survey
D G Andrews

DCTN 52 Mar 1987 The Met O 20 stratosphere-mesosphere model
M Fisher

DCTN 53 Apr 1987 Simulations of linear and nonlinear disturbances in the stratosphere
A O'Neill and V D Pope

DCTN 54 Apr 1987 Aspects of dynamics of the middle atmosphere inferred using data from a satellite and from a numerical model
T D A Fairlie and A O'Neill

DCTN 55 Apr 1987 The seasonal evolution of the stratosphere in the northern hemisphere
A O'Neill and V D Pope

DCTN 56 Apr 1987 The adjustment of numerical weather prediction models to local perturbations
B R Barwell and R A Bromley

DCTN 57 Jun 1987 Climate simulations for 9000 years before present: Seasonal variations and the effect of the Laurentide ice sheet
J F B Mitchell, N S Grahame and K J Needham

DCTN 58 Aug 1987 Climatic effects of nuclear war: the role of atmospheric stability and ground heat fluxes.
J F B Mitchell and A Slingo

DCTN 59 Oct 1987 The stratospheric major warming of winter 1984/85: observations and dynamical inferences.
T D A Fairlie and A O'Neill

DCTN 60 Oct 1987 Some comparisons between the middle atmosphere dynamics of the southern and northern hemispheres
D G Andrews

DYNAMICAL CLIMATOLOGY TECHNICAL NOTES

DCTN 61 Jan 1988 Early winter in the northern stratosphere.
M N Juckes and A O'Neill

DCTN 62 Feb 1988 Single column model tests of the Rowntree convection scheme using GATE data.
D Gregory

DCTN 63 Mar 1988 The antarctic winter; simulations with climatological and reduced sea-ice extents.
J F B Mitchell and C A Senior

DCTN 64 Mar 1988 An investigation of the Gates asynchronous coupling strategy using a simple energy-balance model.
D L Roberts

DCTN 65 Apr 1988 The effect of improved physical parametrizations on simulations of cloudiness and the earth's radiation budget.
A Slingo, R C Wilderspin and R N B Smith

DCTN 66 May 1988 Comparison of data and derived quantities for the middle atmosphere of the southern hemisphere.
W L Grose and A O'Neill

DCTN 67 Aug 1988 Progress and future developments in modelling the climate system with general circulation models.
P R Rowntree

DCTN 68 Aug 1988 A scheme for predicting layer clouds and their water content in a general circulation model.
R N B Smith

DCTN 69 Nov 1988 Modelling climate change: an assessment of sea-ice and surface albedo feedbacks.
W J Ingram, C A Wilson and J F B Mitchell

DCTN 70 Dec 1988 The "greenhouse" effect and climate change
J F B Mitchell

DCTN 71 Dec 1988 On the dependence of climate sensitivity on convective parametrization.
W M Cunnington and J F B Mitchell

DCTN 72 Dec 1988 Land surface parametrizations - basic concepts and review of schemes.
P R Rowntree

DCTN 73 Jan 1989 Climate sensitivity: model dependence of results.
J F B Mitchell

DCTN 74 Jan 1989 Parametrization of the upper ocean mixed layer in a tropical ocean GCM.
S Ineson and C Gordon

DCTN 75 Mar 1989 A simple tropical coupled ocean-atmosphere model.
C R Budin and M K Davey